Effect of Flexible Spacer Length on the Rheology of Side-Chain Liquid-Crystalline Polymers

Kyung Min Lee and Chang Dae Han*

Department of Polymer Engineering, The University of Akron, Akron, Ohio 44325

Received June 2, 2003; Revised Manuscript Received September 5, 2003

ABSTRACT: The effect of flexible spacer length on the rheology of side-chain liquid-crystalline polymers (SCLCPs) was investigated. For the study, a liquid-crystalline monomer, [*n*-[(4-cyanobiphenyl)oxy]alkyl]-carboxylic acid (*n*CN-COOH) with varying methylene groups ($n = 5$, 7, and 11), was grafted onto a nearly monodisperse hydroxylated polyisoprene, yielding SCLCPs, poly{[*n*-[(4-cyanobiphenyl)oxy]alkyl]carbonyl}-oxyisoprenes (PI-*n*CN). Differential scanning calorimetry has shown that the clearing temperature (T_{cl}) of PI-*n*CN increases with increasing *n*. Polarizing optical microscopy has shown that PI-5CN has a nematic mesophase, while both PI-7CN and PI-11CN have a smectic mesophase. The linear dynamic viscoelasticity, steady shear flow, and transient/intermittent shear flows of PI-*n*CN were investigated. It was found that flexible spacer length has a profound influence on the rheological responses of PI-*n*CN. The following observations have been made. (i) At temperatures below T_{cl} the complex viscosity ($|\eta^*|$) of PI-5CN exhibits a very weak frequency dependence, but the frequency dependence of $|\eta^*|$ for PI-*n*CN becomes progressively stronger as the number of methylene spacer groups increases from 5 to 7 and to 11. (ii) The steady-state shear viscosity (η) and first normal stress difference (N_1) of PI-*n*CN decrease as the number of methylene spacer groups increases from 5 to 11. (iii) The η of PI-5CN decreases steadily with increasing temperature without any abnormality as the polymer transforms from the nematic phase to the isotropic phase, whereas the η of both PI-7CN and PI-11CN decreases gradually at $T < T_{cl}$ and then begins to drop precipitously at T_{cl}. (iv) Upon start-up of shear flow, very large overshoot peaks of first normal stress difference growth (N_1^+) and shear stress growth (σ^+) are observed, the extent of which is found to decrease as the number of methylene spacer groups in PI-*n*CN increases from 5 to 11. (v) The recovery time upon cessation of steady shear flow is found to increase as the number of methylene spacer groups in PI-*n*CN increases from 5 to 11.

1. Introduction

There are two types of thermotropic liquid-crystalline polymers (TLCPs): main-chain liquid-crystalline polymers (MCLCPs) and side-chain liquid-crystalline polymers (SCLCPs). During the past two decades a large number of research groups reported on the rheological measurements of MCLCPs. There are too many papers to cite them all here. The readers are referred to some selected papers (refs 1−16 and references therein). One of the practical difficulties with investigating the rheological behavior of MCLCPs, especially commercial MCLCPs, lies in that in general they have very high melting and clearing temperatures, leading one easily to encounter the possibility of having thermal degradation during rheological measurement in the liquid-crystalline state. To overcome the difficulty, in the 1980s some serious efforts[17−21] were made on the synthesis of "semiflexible" or "segmented" MCLCPs by placing flexible spacer groups, typically methylene groups, between phenyl rings in the polymer backbone. Such efforts were summarized in a review article by Ober et al.[22] Having realized that the presence of flexible spacers in the polymer backbone lowers the melting temperature, but not the clearing temperature of segmented MCLCPs, some research groups[23−25] developed synthesis procedures to lower both melting and clearing temperatures by attaching a pendant group(s) onto the rigid polymer backbone. Indeed, such synthesis procedures have been very successful at lowering both the melting and clearing temperatures of segmented MCLCPs much below the thermal degradation temperature. Such successful efforts enabled some researchers[5−11] to investigate the rheological behavior of segmented MCLCPs with bulky arylsulfonyl pendant group and others[12] to investigate the effect of bulkiness of pendant groups on the rheological behavior of segmented MCLCPs in the liquid-crystalline state without encountering the possibility of having thermal degradation.

In the 1980s, a number of research groups reported on the syntheses of SCLCPs and such efforts were summarized in a review article by Shibaev and Platé[26] in 1984 and in a monograph by McArdle[27] in 1989. In the 1990s, many research groups[28−52] continued to synthesize SCLCPs and then investigated thermal transitions and mesophase structures. During the same period some activities on the rheological investigation of SCLCPs were reported.[53−66] It can easily be surmised that the architecture of polymers, SCLCP vs MCLCP, would have a profound influence on their rheological behavior, leading us to speculate that there might be some fundamental differences in the rheological behavior between MCLCP and SCLCP. Indeed, in our previous paper,[66] we compared the rheological behavior of a segmented MCLCP with that of a SCLCP. Needless to state, although such a comparison revealed some interesting observations, a generalization of the comparison, based on the particular study, to all MCLCPs and SCLCPs may not be warranted because there are so many different chemical structures that exhibit a variety of liquid crystallinities in SCLCPs. A comparison of the rheological behavior between SCLCPs and MCLCPs is complicated by the differences in mesophase structures. Specifically, almost all MCLCPs employed for the rheological investigations in the past had a nematic mesophase. Only a few studies[12,13] reported on the rheological behavior, over a very narrow range of temperatures, of MCLCPs forming smectic mesophases

10.1021/ma030303o CCC: $25.00
Published on Web 10/22/2003

Scheme 1

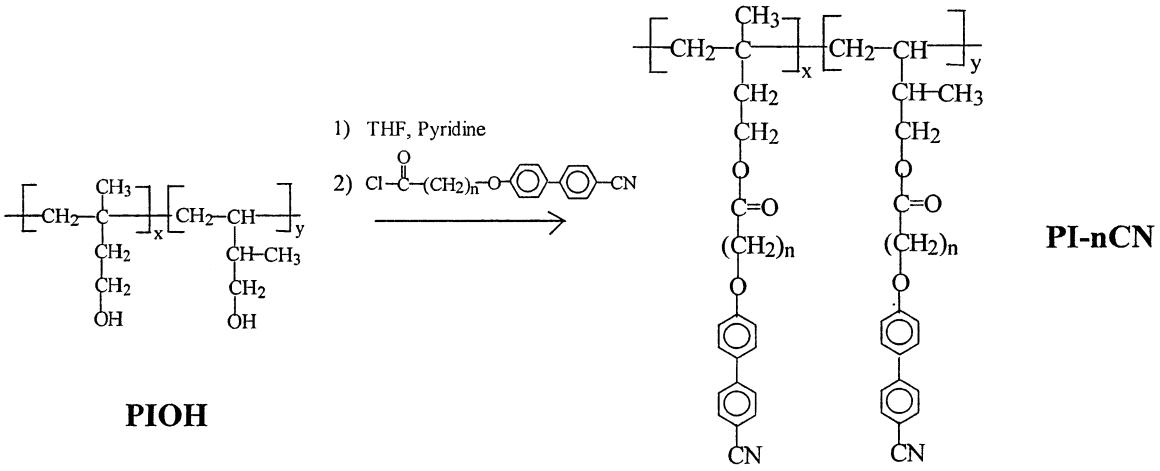

because they are extremely viscous in the liquid-crystalline state. The readers are reminded that smectic mesophases have two-dimensional layered structures and there are several different forms of smectics.

On the other hand, several studies[53,55,58,61,64] reported on the rheological behavior, over a wide range of temperatures, of SCLCPs having a smectic mesophase. Basically, SCLCP consists of three parts: polymer backbone, side-chain liquid-crystalline (LC) monomers, and flexible spacer groups that connect the polymer backbone and side-chain LC monomers. It has been found that many SCLCPs have clearing temperatures far below their thermal degradation temperatures, allowing one to conduct rheological investigations in the liquid-crystalline state without encountering the possibility of having thermal degradation. It has also been found that SCLCPs having short flexible spacer groups tend to form a nematic mesophase, while SCLCPs having long flexible spacer groups tend to form a smectic mesophase. The above observations suggest that the liquid crystallinities (nematics and smectics), and hence the rheological behavior, of SCLCPs depend not only on the chemical structures of the side-chain LC monomers but also on the length of flexible spacer groups. However, to date, little has been reported on the effect of flexible spacer length in SCLCPs on the rheological responses to transient shear flow, intermittent shear flow, steady shear flow, oscillatory shear flow, and stress relaxation upon cessation of steady shear flow.

In our previous paper,[66] we reported on the rheological behavior of a nematic-forming model SCLCP that had a polyisoprene backbone, onto which LC monomers with 5 methylene spacer groups were grafted. Having observed some unexpected rheological behavior of this SCLCP as compared to a segmented MCLCP, in the present study we synthesized two additional SCLCPs of the same moieties by increasing the number of methylene spacer groups from 5 to 7 and to 11 and then investigated their rheological behavior. We found that these two new SCLCPs exhibit a smectic mesophase, in contrast to the nematic SCLCP employed in our previous study.[66] In the present study, using these SCLCPs, we investigated the rheological responses to transient shear flow, intermittent shear flow, steady shear flow, and oscillatory shear flow, and also time evolution of dynamic storage and loss moduli upon cessation of steady shear flow by applying very small-amplitude oscillatory deformation. Our primary objective of the study was to investigate the effect of flexible spacer length on the rheological responses of the SCLCPs. We have made some very interesting, unexpected observations from this study. Thus, in this paper we report the highlights of our findings.

2. Experimental Section

Synthesis of LC Monomers and SCLCPs. We first synthesized, via anionic polymerization in tetrahydrofuran (THF) as solvent, polyisoprene (PI) having a number-average molecular weight (M_n) of 1.43×10^4 as determined by membrane osmometry (Jupiter Instrument) and a polydispersity index (M_w/M_n) of 1.05 as determined by gel permeation chromatography (GPC, Waters). Subsequently, the PI was hydroxylated, via hydroboration/oxidation reactions, to obtain a nearly monodisperse hydroxylated PIOH. The details of the hydroboration/oxidation procedures employed are described in the literature.[67−69] In the present study, we employed THF as solvent in the polymerization of isoprene, which resulted in PI having the following microstructures: 34% 1,2-addition, 59% 3,4-addition, and 7% 1,4-addition. If isoprene is polymerized in cyclohexane, the resulting PI would have 94% 1,4-addition and 6% 3,4-addition. According to Chung et al.,[68] the rate of hydroboration/oxidation reactions, which convert the double bonds in PI to hydroxyl groups, is much faster with the PI having high vinyl contents (1,2- and 3,4-addition) than with the PI having high 1,4-addition.

Three liquid-crystalline monomers, [*n*-[(4-cyanobiphenyl)-oxy]alkyl]carboxylic acid (*n*CN-COOH), with the chemical structure

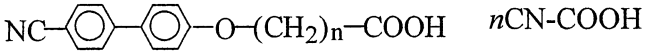

with $n = 5$, 7, and 11 were synthesized, where n denotes the number of methylene groups. Hereafter, this structure will be referred to as *n*CN-COOH. Subsequently, *n*CN-COOH was chlorinated to obtain *n*CN-COCl. The details of the synthesis of *n*CN-COOH and chlorination procedures are described in our previous paper.[66] The grafting of *n*CN-COCl onto the PIOH was accomplished by the reaction route shown in Scheme 1.

An accurate determination of the molecular weight of PI-*n*CN from the GPC trace was not possible since information on the hydrodynamic volume of PI-*n*CN was unavailable. Therefore, we calculated the molecular weight of PI-*n*CN using information on the degree of hydroxylation. The estimated molecular weight and the polydispersity index, determined from GPC, of PI-5CN, PI-7CN, and PI-11CN are given in Table 1. The chemical structures of the three liquid-crystalline monomers and three SCLCPs (PI-5CN, PI-7CN, and PI-11CN) synthesized were confirmed using ^{1}H nuclear magnetic resonance (NMR) spectroscopy and Fourier transform infrared (FTIR) spectroscopy. For such purposes, both ^{13}C and ^{1}H NMR spectra were obtained using a spectrometer (Varian Gemini-

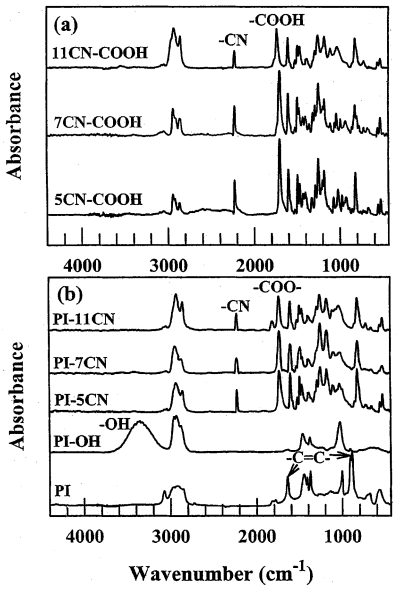

Figure 1. (a) FTIR spectra for 5CN-COOH, 7CN-COOH, and 11CN-COOH. (b) FTIR spectra for PI, PI-OH, PI-5CN, PI-7CN, and PI-11CN.

Table 1. Molecular Characteristics of the SCLCPs Synthesized in This Study

sample code	M_n	M_w/M_n [a]	structure
PI	1.43×10^4 [b]	1.05	polyisoprene backbone
PI-5CN	7.19×10^4 [c]	1.08	PI with 5CN-COOH
PI-7CN	7.78×10^4 [c]	1.07	PI with 7CN-COOH
PI-11CN	8.80×10^4 [c]	1.08	PI with 11CN-COOH

[a] Determined from GPC. [b] Determined from membrane osmometry. [c] Calculated value based on the degree of hydroxylation.

200, 200 MHz). Because of space limitations, NMR spectra for the materials are not presented here.

Fourier Transform Infrared (FTIR) Spectroscopy. The chemical structures of the three LC monomers and three SCLCPs synthesized were characterized using Fourier transform infrared (FTIR) spectroscopy. Films suitable for FTIR spectroscopy were prepared by casting 2% (w/v) solution in THF or chloroform directly on the KBr salt plate. Film thickness was adjusted, such that the maximum absorbance of any band was less than 1.0, at which the Beer−Lambert law is valid. It was slowly dried for 24 h in a fume hood until most of the solvent evaporated and then dried at 70 °C for a few days in a vacuum oven. Samples were then stored under vacuum until use. FTIR spectra were obtained using a Perkin-Elmer spectrometer (model 16PC FTIR). Spectral resolution was maintained at 4 cm^{-1}. Figure 1a gives FTIR spectra for 5CN-COOH, 7CN-COOH, and 11CN-COOH, showing the presence of −CN and −COOH bands. Figure 1b gives FTIR spectra for PI, PI-OH, PI-5CN, PI-7CN, and PI-11CN. It is seen in Figure 1b that few (if any) double bonds are discernible in the PI-OH, with hydrogen-bonded hydroxyl groups at 3330 cm^{-1}. It is clearly seen from the FTIR spectra for PI-5CN, PI-7CN, and PI-11CN in Figure 1b that all the double bonds at 1640 and 910 cm^{-1} in the PI have been hydroxylated. Also, coupling reactions between PI-OH and 5CN-COCl, 7CN-COCl, or 11CN-COCl have been completed, as indicated by the ester (−COO−) peak at 1730 cm^{-1} and the −CN peak at 2230 cm^{-1}. Notice in Figure 1b that no hydroxyl groups are present in the PI-5CN, PI-7CN, and PI-11CN.

Differential Scanning Calorimetry (DSC). Thermal transition temperatures of all specimens were determined using DSC (Perkin-Elmer 7 series), under a nitrogen atmosphere, at a heating rate of 20 °C/min. The DSC traces for 5CN-COOH, 7CN-COOH, and 11CN-COOH are given in Figure 2a, which show that (1) 5CN-COOH has a clearing temperature (T_{cl}) of 168 °C, 7CN-COOH has a T_{cl} of 146 °C,

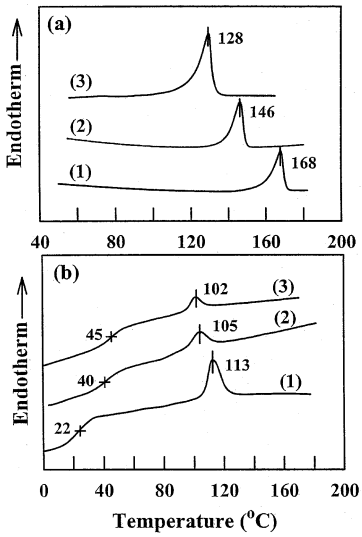

Figure 2. (a) DSC traces of (1) 5CN-COOH, (2) 7CN-COOH, and (3) 11CN-COOH. (b) DSC traces of (1) PI-11CN, (2) PI-7CN, and (3) PI-5CN, which were obtained in the second heating at a rate of 20 °C/min.

and (3) 11CN-COOH has a T_{cl} of 128 °C. It is interesting to observe in Figure 2a that T_{cl} decreases as the number of methylene groups increases from 5 to 11. We attribute such high values of T_{cl} for *n*CN-COOH to the presence of hydrogen bonds of carbonyl group as evidenced from the FTIR spectra (see Figure 1a), showing that, among the three LC monomers, 5CN-COOH exhibits the strongest intensity, while 11CN-COOH has the weakest intensity, of the ester (−COO−) peak at 1730 cm^{-1}. Figure 2b gives DSC traces for PI-5CN, PI-7CN, and PI-11CN, showing that (1) PI-11CN has a glass transition temperature (T_g) of 22 °C and a T_{cl} of 113 °C, (2) PI-7CN has a T_g of 40 °C and a T_{cl} of 105 °C, and (3) PI-5CN has a T_g of 45 °C and a T_{cl} of 102 °C. It is interesting to observe in Figure 2b that T_{cl} increases, while T_g decreases, as the number (n) of methylene groups in PI-*n*CN increases.

Polarizing Optical Microscopy (POM). A hot-stage (TH-600 type, Linkham Scientific) microscope (Nikon, model Optiphoto polXTP-11) with a camera, a programmable temperature controller, and photomicrographic attachment was used to obtain images under cross-polarized light. Specimens were cast from THF (1 wt % solution) on a slide glass to obtain a film sample of about 2−3 μm in thickness, which was then dried first in a fume hood and then in a vacuum oven. Figure 3 gives POM images of 5CN-COOH, 7CN-COOH, and 11CN-COOH, which were taken during the cooling cycle, showing that 5CN-COOH has two and four brushes, suggesting that 5CN-COOH has a nematic phase, and both 7CN-COOH and 11CN-COOH have a smectic mesophase. Figure 3 also gives POM images of PI-5CN, PI-7CN, and PI-11CN, which were taken during the cooling cycle, showing that PI-5CN has a nematic phase, while both PI-7CN and PI-11CH have a smectic mesophase. That is, the mesophase structure of *n*CN-COOH does not change, even after it was grafted on the PI main chain. Earlier, Wewerka et al.[64] made a similar observation on two SCLCPs, C5 and C9, in which norbonene formed the main chain onto which 5CN-COOH or 9CN-COOH was grafted; namely, C5 having 5CN-COOH as side chain had a nematic mesophase and C9 having 9CN-COOH as side chain had a smectic mesophase.

Rheological Measurements. Specimens for rheological measurements were prepared by first dissolving each polymer in THF in the presence of 0.1 wt % antioxidant (Irganox 1010, Ciba-Geigy Group) and then slowly evaporating the solvent at room temperature for 1 week. The cast films (1 mm thick) were further dried in a vacuum oven at room temperature for at least 3 weeks and, prior to measurements, at 60 °C for 48 h to remove any residual solvent and moisture. The very slow drying of the cast films at room temperature for 3 weeks was

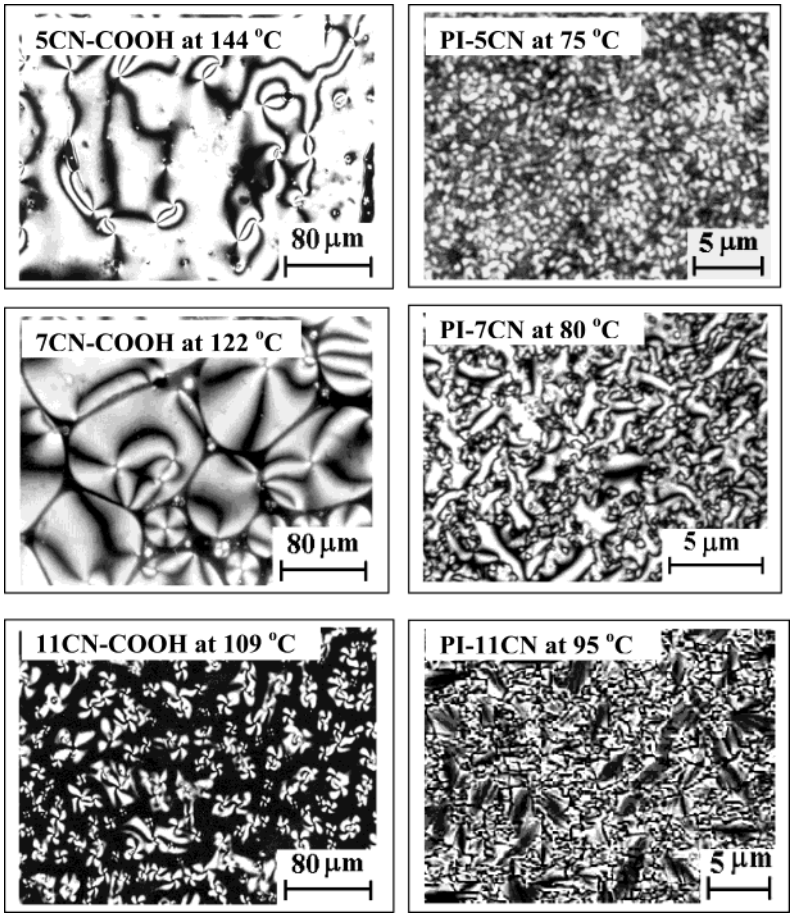

Figure 3. POM images of 5CN-COOH at 144 °C, PI-5CN at 75 °C, 7CN-COOH at 122 °C, PI-7CN at 80 °C, 11CN-COOH at 109 °C, and PI-11CN at 95 °C.

adopted in order to avoid the possibility of encountering bubble formation, which would be detrimental to obtain reproducible rheological data. An Advanced Rheometric Expansion System (ARES, Rheometric Scientific) with a parallel-plate (8 mm diameter plate) fixture, with gap opening being set to 0.8 mm, was employed to conduct oscillatory shear experiments in order to measure the dynamic storage and loss moduli (G' and G'') of each PI-*n*CN synthesized as functions of angular frequencies (ω) in the range from 0.04 to 100 rad/s. Only after we ascertained that the normal force signal reached the baseline did we commence oscillatory shear experiments. Using such a protocol, we were able to obtain reproducible data. In the oscillatory shear measurements a fixed strain of 0.04 was used to ensure that measurements were taken well within the linear viscoelastic range of the materials investigated. The frequency sweep experiment at a preset temperature lasted for about 45 min. Further, values of G' and G'' were monitored at $\omega = 1$ rad/s after waiting a predetermined period upon cessation of steady shear flow. A cone-and-plate (8 mm diameter plate, 0.1 rad cone angle) fixture, with gap opening at the apex of the cone and plate being set to 50 μm, was used to investigate transient shear flow, intermittent shear flow, and steady-state shear flow. For the transient and intermittent shear flows, both shear stress growth (or decay) and first normal stress difference growth (or decay) were recorded as functions of time at three different shear rates ($\dot{\gamma}$): 0.1, 0.5, and 1.0 s^{-1}. An intermittent shear flow experiment was conducted after waiting for a predetermined period upon cessation of steady shear flow. The experimental protocols employed for the transient and steady-state shear experiments were virtually the same as that for the oscillatory shear experiments described above, except for that the gap setting of the cone-and-plate fixture was 50 μm. Only after we ascertained that the normal force signal reached the baseline did we commence transient shear flow (until steady state was reached). Using such a protocol, we were able to obtain reproducible data. Temperature control was satisfactory to within ±1 °C. All experiments were conducted under a nitrogen atmosphere to minimize oxidative degradation of the specimens.

3. Results and Discussion

Linear Dynamic Viscoelasticity. Figure 4 gives log G' vs log ω plots for (a) PI-5CN, (b) PI-7CN, and (c) PI-11CN at various temperatures. The following observations are worth noting in Figure 4. Over the entire range of ω tested the slope of log G' vs log ω plots for PI-5CN is slightly less than 2 at temperatures below ca. 105 °C and then becomes 2 when the temperature is increased to 105 °C and higher. This temperature is close to the T_{cl} (102 °C) of PI-5CN determined from DSC (see Figure 2b). The frequency dependence of G' shown in Figure 4a makes sense because at temperatures below T_{cl} PI-5CN has a nematic mesophase (see Figure 3) and at temperatures (T) above T_{cl} PI-5CN forms a homogeneous phase. Thus, the log G' vs log ω plots having a slope of 2 in the terminal region of PI-5CN at $T \geq T_{cl}$ exhibit liquidlike behavior because the PI backbone of PI-5CN is nearly monodisperse. As can be seen from Figure 4b, the log G' vs log ω plots in the terminal region of PI-7CN have a slope much less than 2 at $T < 100$ °C, but the slope begins to change at 105 °C and becomes 2 at $T \geq 110$ °C in the isotropic state. Figure 4c shows that at $T < 105$ °C PI-11CN exhibits solidlike behavior having a very small slope in the log G' vs log ω plots, and then it exhibits liquidlike behavior at $T \geq 115$ °C and a slope of 2. It is clear from Figure 4 that in the terminal region at $T < T_{cl}$ the frequency dependence of log G' vs log ω plots of PI-*n*CN exhibits progressively stronger solidlike behavior as the number of methylene

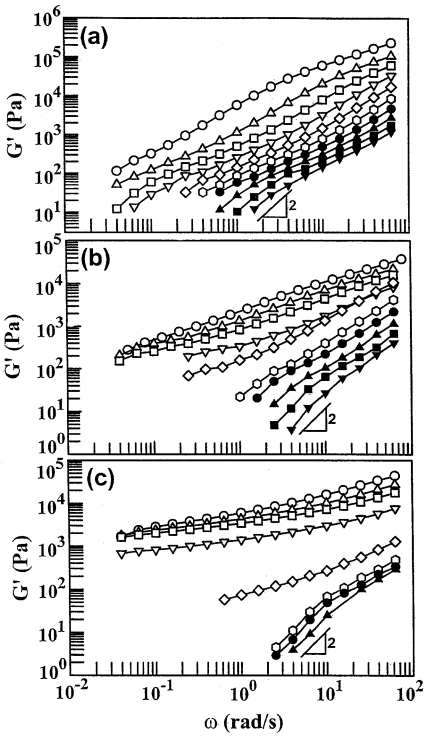

Figure 4. Plots of log G' vs log ω for (a) PI-5CN at (○) 75, (△) 80, (□) 85, (▽) 90, (◇) 95, (⬠) 100, (●) 105, (▲) 110, (■) 115, and (▼) 120 °C; (b) PI-7CN at (○) 80, (△) 85, (□) 90, (▽) 95, (◇) 100, (⬠) 105, (●) 110, (▲) 115, (■) 120, and (▼) 125 °C; and (c) PI-11CN at (○) 80, (△) 90, (□) 100, (▽) 105, (◇) 110, (⬠) 115, (●) 120, and (▲) 125 °C.

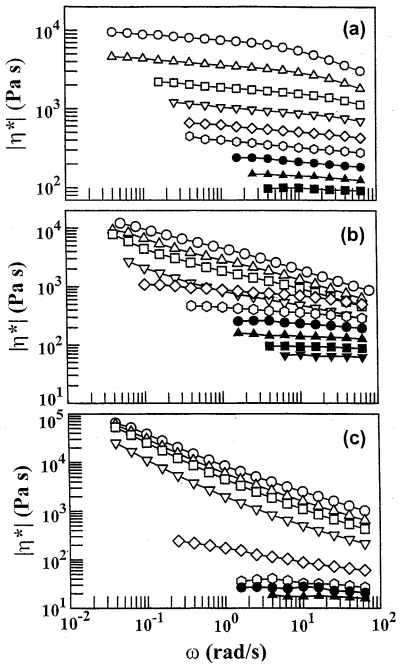

Figure 5. Plots of log $|\eta^*|$ vs log ω for (a) PI-5CN at (○) 75, (△) 80, (□) 85, (▽) 90, (◇) 95, (⬠) 100, (●) 105, (▲) 110, (■) 115, and (▼) 120 °C; (b) PI-7CN at (○) 80, (△) 85, (□) 90, (▽) 95, (◇) 100, (⬠) 105, (●) 110, (▲) 115, (■) 120, and (▼) 125 °C; and (c) PI-11CN at (○) 80, (△) 90, (□) 100, (▽) 105, (◇) 110, (⬠) 115, (●) 120, and (▲) 125 °C.

spacer groups increases from 5 to 11. This observation is attributable to an increase in the strength of mesogenics as the number of methylene spacer groups in PI-*n*CN increases from 5 to 11. Notice further in Figure 4 that at the same distance from the T_{cl} of each polymer, at $T_{cl} - T$, in the anisotropic region the magnitude of G' in the terminal region has the following order: G'(PI-11CN) > G'(PI-7CN) > G'(PI-5CN).

Figure 5 gives log $|\eta^*|$ vs log ω plots for (a) PI-5CN, (b) PI-7CN, and (c) PI-11CN at various temperatures, where $|\eta^*|$ is complex viscosity defined by $|\eta^*| = [(G'/\omega)^2 + (G''/\omega)^2]^{1/2}$. The following observations are worth noting in Figure 5. In Figure 5a, the log $|\eta^*|$ vs log ω plots for PI-5CN show a very weak frequency dependence even at $T < T_{cl}$ (102 °C), and then they begin to show Newtonian behavior at $T \geq 110$ °C. In Figure 5a, we do not observe a temperature at which an abrupt change in the frequency dependence of log $|\eta^*|$ vs log ω plots for PI-5CN occurs; i.e., a smooth transition takes place from very weak frequency dependence in the nematic state to frequency independence in the isotropic state. In Figure 5b, we observe that log $|\eta^*|$ vs log ω plots for PI-7CN have a strong frequency dependence at $T \leq 95$ °C, a very mild frequency dependence at 105 °C, and then Newtonian behavior at $T \geq 110$ °C. Similarly, in Figure 5c we observe that log $|\eta^*|$ vs log ω plots for PI-11CN have a very strong frequency dependence at $T \leq 105$ °C, a very mild frequency dependence at 110 °C, and then Newtonian behavior at $T \geq 115$ °C. We can conclude from Figure 5 that the frequency dependence of log $|\eta^*|$ vs log ω plots at $T < T_{cl}$ becomes increasingly stronger as the number of methylene spacer groups in PI-*n*CN increases from 5 to 7 and to 11. A strong frequency dependence of $|\eta^*|$ at low angular frequencies in oscillatory shear flow is believed to be characteristic of multiphase polymeric liquids, including highly filled molten polymers,[70] MCLCPs,[12,71] and microphase-separated block copolymers.[72,73] What seems very peculiar, however, in Figure 5 is that the nematic-forming PI-5CN at $T < T_{cl}$ exhibits a very weak frequency dependence of $|\eta^*|$ over the entire range of angular frequencies tested, behavior often observed in ordinary flexible polymers, while the smectic-forming PI-7CN and PI-11CN at $T < T_{cl}$ exhibit a very strong frequency dependence of $|\eta^*|$ at low angular frequencies. We defer further discussion of this observation until we present below the rheological responses of the three PI-*n*CNs in steady-state shear flow.

Figure 6 gives log G' vs log G'' plots for (a) PI-5CN, (b) PI-7CN, and (c) PI-11CN at various temperatures. The following observations are worth noting in Figure 6. The log G' vs log G'' plots (Figure 6a) for PI-5CN show a very weak temperature dependence over the entire range of temperatures tested below and above T_{cl} (102 °C as determined from DSC). On the other hand, the log G' vs log G'' plots (Figure 6b) for PI-7CN show temperature dependence at $T < 110$ °C, but they become independent of temperature at $T \geq 110$ °C and have a slope of 2 in the terminal region. Similar observations can be made from Figure 6c for PI-11CN; namely log G' vs log G'' plots show a temperature dependence at $T \leq 110$ °C, but they become independent of temperature at $T \geq 115$ °C and have a slope of 2 in the terminal region. Notice that the temperature at which log G' vs log G'' plots for both PI-7CN and PI-11CN begin to become independent of temperature is very close to the T_{cl} determined from DSC for the respective SCLCPs (see Figure 2b). Thus log G' vs log G'' plots for SCLCPs may be useful to determine T_{cl}. This is not surprising in that log G' vs log G'' plots have extensively been used to determine the order−disorder transition temperature (T_{ODT}) of cylinder- and lamella-forming block copolymers.[74−76] However, a question remains to be

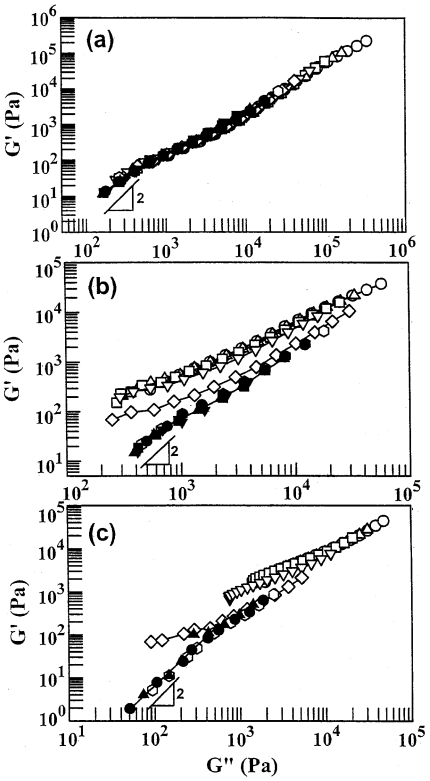

Figure 6. Plots of log G' vs log G'' for (a) PI-5CN at (○) 75, (△) 80, (□) 85, (▽) 90, (◇) 95, (⬡) 100, (●) 105, (▲) 110, (■) 115, and (▼) 120 °C; (b) PI-7CN at (○) 80, (△) 85, (□) 90, (▽) 95, (◇)100, (⬡) 105, (●) 110, (▲) 115, (■) 120, and (▼) 125 °C; and (c) PI-11CN at (○) 80, (△) 90, (□) 100, (▽) 105, (◇) 110, (⬡) 115, (●) 120, and (▲) 125 °C.

answered: Why do the log G' vs log G'' plots for PI-5CN (Figure 6a) show a very weak temperature dependence over the entire range of temperatures tested from 75 °C (below T_{cl}) to 120 °C (above T_{cl}), while the log G' vs log G'' plots for PI-7CN and PI-11CN show a distinct temperature dependence at $T < T_{cl}$? At present, we can only offer the following speculative explanation to this question: (i) the nematics in PI-5CN may be very weak while the smectics in PI-7CN and PI-11CN are very strong, and (ii) five methylene spacer groups in PI-5CN may not be sufficiently long to decouple the side-chain liquid-crystalline monomers from the polymer backbone. When the number of methylene spacer groups is increased sufficiently, yielding PI-7CN and PI-11CN, the side-chain liquid-crystalline monomers form layered structures and the motions of side-chain LC monomers may be decoupled from the motions of polymer backbone.

At this juncture it seems quite appropriate to mention the earlier study of Wewerker et al.,[64] who also investigated linear dynamic viscoelasticity of two SCLCPs, one (C5-low) having five methylene spacer groups and the other (C9-low) having nine methylene spacer groups. Both C5-low and C9-low had the same LC monomers [*n*-[(4-cyanobiphenyl)oxy)]alkyl]carboxylic acids as the PI-*n*CNs employed in the present study, but the backbone of C5-low and C9-low was poly(norbonenedicarboxylic acid), while the backbone of PI-*n*CNs is polyisoprene. In presenting their experimental results, Wewerker et al.[64] employed time−temperature superposition (TTS) to obtain so-called master curves, log G' vs log $a_T\omega$ plots, with a_T being a temperature-dependent shift factor obtained empirically, for both C5-low and C9-low over the entire range of temperatures tested using 40 °C as a reference temperature (T_{ref}). Note that the reference temperature chosen was below the T_{cl} of C5-low and C9-low. It should be pointed out that an application of TTS to C5-low and C9-low is not warranted as long as they are in the anisotropic region (i.e., at $T < T_{cl}$). As a matter of fact, Wewerker et al.[64] obtained different temperature dependences of a_T for three separate ranges of temperature, clearly demonstrating the failure of TTS for their SCLCPs, C5-low and C9-low. On the other hand, the preparation of log G' vs log G'' plots (see Figure 6) does not require any manipulation of experimental data; i.e., no shift factor is needed! The log G' vs log $a_T\omega$ plots in the terminal region of C5-low (Figure 6 in ref 64) show a temperature dependence at $T < T_{cl}$ (97 °C) but a temperature independence at $T \geq T_{cl}$ with a slope less than 2.

It is very clear from Figure 6b,c that there is no way one can obtain temperature-independent reduced plots, log G' vs log $a_T\omega$ and log G'' vs log $a_T\omega$ plots, for PI-7CN and PI-11CN by shifting log G' vs log ω and log G'' vs log ω plots along the ω axis (i.e., TTS would fail!). Rheologically speaking, SCLCPs at $T < T_{cl}$ are of no or little difference from microphase-separated block copolymers or two-phase polymer blends. Under such circumstances, TTS is expected to fail except when the relaxation times for the two phases (the mesophase and the isotropic phase) in an SCLCP have an identical temperature dependence, which would rarely occur in real systems. In other words, as long as the temperature dependence of the relaxation time of the mesophase in an SCLCP is different from that of the isotropic phase, an application of TTS to the SCLCP is not warranted. Notice in Figure 6 that log G' vs log G'' plots at $T \geq T_{cl}$ are independent of temperature and have a slope of 2 in the terminal region, behavior often observed in monodisperse or nearly monodisperse flexible homopolymers. Thus, an application of TTS to SCLCPs at $T \geq T_{cl}$ (in the isotropic state) is warranted.

Two comments are worth making regarding the log G' vs log $a_T\omega$ plots for C5-low (Figure 6 in ref 64) and the log G' vs log G'' plots for PI-5CN (Figure 6a). C5-low shows a strong temperature dependence of log G' vs log $a_T\omega$ plots at $T < T_{cl}$, while PI-5CN shows a very weak temperature dependence of log G' vs log G'' plots at $T < T_{cl}$. We attribute this difference between the two SCLCPs to the differences in the chemical structures of the polymer backbones, polyisoprene in PI-5CN and poly(norbonenedicarboxylic acid) in C5-low. The observation that C5-low had a slope less than 2 in the terminal region of log G' vs log $a_T\omega$ plots at $T > T_{cl}$ (Figure 6 in ref 64) is attributable to the polydisperse nature of C5-low. Wewerker et al. could have observed a slope of 2 in the terminal region of log G' vs log $a_T\omega$ plots at $T > T_{cl}$ if they had applied much lower angular frequencies (say as low as 10^{-4} rad/s) than the lowest angular frequency applied in their experiment. According to Wewerker et al.,[64] C5-low was obtained using ring-opening metathesis polymerization and had a polydispersity index of 1.4. On the other hand, the log G' vs log G'' plots of PI-5CN, PI-7CN, and PI-11CN at $T > T_{cl}$ have a slope of 2 in the terminal region (see Figure 6) because the PI-*n*CNs are nearly monodisperse polymers having polydispersity indices less than 1.1 (see Table 1). Note that the polymer backbone PI of PI-*n*CNs was synthesized using anionic polymerization, and then liquid-crystalline monomers with methylene spacer groups were grafted onto the polymer backbone. It is

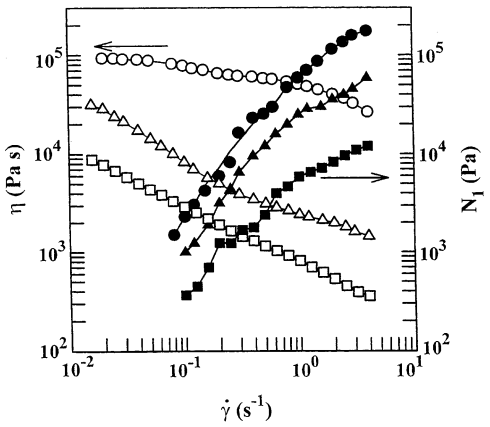

Figure 7. Plots of log η vs log $\dot{\gamma}$ (open symbols) and log N_1 vs log $\dot{\gamma}$ (filled symbols) for PI-5CN at 70 °C (○, ●), PI-7CN at 75 °C (△, ▲), and PI-11CN at 90 °C (□, ■).

well documented in the literature[77−79] that the log G' vs log G'' plots of monodisperse homogeneous polymers (e.g., monodisperse TLCPs at $T > T_{cl}$) are expected to have a slope of 2 in the terminal region.

In their second paper, Wewerker et al.[65] presented log G' vs log G'' plots for H3 and H9, similar to Figure 6 presented above. Note that the chemical structures of H3 (having three methylene spacer groups) and H9 (having nine methylene spacer groups) are exactly the same as those of C5-low and C9-low employed in their earlier paper.[64] The log G' vs log G'' plots for H3 and H9 in the terminal region (Figures 3 and 5 in ref 65) at $T \geq T_{cl}$ have a slope less than 2, while the log G' vs log G'' plots for PI-5CN, PI-7CN, and PI-11N (Figure 6) in the terminal region at $T \geq T_{cl}$ have a slope very close to 2. This is because H3 had a polydispersity index of 1.44 and H9 had a polydispersity index of 1.58,[65] while the three PI-*n*CNs in Figure 6 are nearly monodisperse polymers having polydispersity indices less than 1.1 (see Table 1).

Steady-State Shear Flow Properties. Figure 7 gives logarithmic plots of steady-state shear viscosity (η) vs shear rate ($\dot{\gamma}$) and logarithmic plots of steady-state first normal stress difference (N_1) vs $\dot{\gamma}$ for PI-5CN at 70 °C, PI-7CN at 75 °C, and PI-11CN at 90 °C, all in the anisotropic region, for $\dot{\gamma}$ ranging from 0.01 to 7 s^{-1}. We have chosen different measurement temperatures for each polymer, so that a comparison of η and N_1 among the three polymers can be made at approximately the same distance from the T_{cl} of each polymer, i.e., at $T_{cl} - T$. The rationale behind this approach lies in that a comparison of the rheological properties of TLCPs at $T_{cl} - T$ would minimize, if not eliminating completely, the effect of molecular weight because T_{cl} reflects the chemical structures of polymers and, also, depends on their molecular weights.[7] Earlier, Chang and Han[11] showed that the choice of $T_{cl} - T$ minimizes the effect of molecular weight of MCLCPs on η. In Figure 7 there does not exist three distinct regions of steady-state shear viscosity, noted earlier by Onogi and Asada,[80] for all three PI-*n*CNs. Specifically, PI-5CN does not exhibit shear-thinning behavior at low shear rates (i.e., no region I); instead, it exhibits a constant shear viscosity at low shear rates (region II) and then weak shear-thinning behavior at high shear rates (region III). On the other hand, PI-7CN and PI-11CN exhibit very strong shear-thinning behavior over the entire range of shear rates tested, i.e., region I followed by region III, without having region II between regions I and III. Such steady-state viscosity behavior has also been observed in MCLCPs,[2,3,6,15] microphase-separated block copolymers,[73] and highly filled molten polymers.[70] Note that in the anisotropic region (at $T < T_{cl}$) of all three PI-*n*CNs the shear-rate dependence of η in steady shear flow (Figure 7) is very similar qualitatively to the angular frequency dependence of $|\eta^*|$ in oscillatory shear flow (Figure 5).

Referring to Figure 7, the following questions may be raised: Why does PI-5CN exhibit the shear rate dependence of steady-state viscosity very similar to that of high-molecular-weight ordinary flexible polymers? What is the origin(s) of the strong shear-thinning behavior of steady-state viscosity especially at low shear rates in PI-7CN and PI-11CN? These two questions are not mutually exclusive. It is generally agreed among researchers that the origin of the shear-thinning behavior at low shear rates (region I) in TLCPs may arise from the presence of a piled polydomain texture, composed of mesogenics possessing little or no macroscopic flow-induced orientation. Interestingly, however, from viscosity measurements for lyotropes of various concentrations of poly(γ-benzyl L-glutamate) in *m*-cresol, Ugaz et al.[81] observed region I in steady-state shear viscosity only for ca. 35 wt % and higher concentrations and then concluded that region I shear-thinning behavior may not be universally expected in all nematic LCPs.

At present, we are not certain of the origin that gives rise to the steady-state shear flow responses (N_1 and η in Figure 7) of PI-5CN very similar to those of high-molecular-weight ordinary flexible polymers. As will be shown below, the transient shear responses of PI-5CN are distinctly different from those of high-molecular-weight ordinary flexible polymers. Earlier, Imrie et al.[36] synthesized a series of SCLCPs by reacting α-bromo-ω-(4-methoxyazobenzene-4′oxy)alkane with poly(4-hydroxystyrene) by varying the number of methylene spacer groups ranging from 3 to 12. They found that the polymer having three methylene spacer groups did not exhibit liquid crystallinity, while the polymers having higher methylene spacer groups had smectic mesophase. At present, there is no theory that predicts a minimum number of methylene spacer groups required to exhibit liquid crystallinity in SCLCPs. The minimum number of methylene spacer groups required to exhibit liquid crystallinity in SCLCPs would depend on the chemical structures of the polymer backbone and side-chain liquid-crystalline monomers. It is then possible that the number of methylene spacer groups in PI-5CN, though forming nematic mesophase, is not sufficiently large, giving rise to the shear-rate dependence of steady-state viscosity similar to that of high-molecular-weight ordinary flexible polymers.

Notice in Figure 7 that values of N_1 for all three PI-*n*CNs are positive over the entire range of $\dot{\gamma}$ tested, similar to the previous studies on MCLCPs.[4−12,14,16] In the past, a number of research groups[82−88] reported experimental results of negative N_1 in main-chain lyotropes, but little, if any, experimental evidence has been reported on negative N_1 in TLCPs. The origin of negative N_1 in main-chain lyotropes has been explained theoretically.[89−91] Today it is well accepted that sign changes in N_1 in steady-state shear flow are intimately related to tumbling in main-chain lyotropes. However, at present there is no theory suggesting that TLCPs would necessarily show negative N_1 if they were tumbling. Thus, one may argue that an experimental

observation of positive N_1 in steady-state shear flow of TLCPs may not be sufficient for one to conclude that they exhibit flow aligning behavior. In this regard, two recent studies are worth mentioning. Using in situ X-ray scattering on an MCLCP (PSHQ6−12) that gives rise to positive N_1 in steady shear flow, Ugaz and Burghardt[92] concluded that the MCLCP was flow aligning. Using in-situ flow conoscopy on an MCLCP (DHMS-7,9) that gives rise to positive N_1 in steady shear flow, Zhou et al.[93] concluded that the MCLCP was flow aligning. It appears at least from an experimental point of view that there exists a correlation between positive N_1 and flow aligning behavior in MCLCPs. However, such a correlation does not seem to exist yet for SCLCPs. Earlier, Quijada-Garrido et al.[62,63] conducted transient shear flow experiments on SCLCPs and concluded that their polymers exhibited tumbling on the basis of the observations made on oscillations of $N_1^+(\dot{\gamma},t)$ during transient shear flow. Below we will address this issue.

What is of great interest in Figure 7 is that, at given values of $\dot{\gamma}$, both η and N_1 decrease as the number of methylene spacer groups in PI-*n*CN increases, although the molecular weight of PI-*n*CN increases slightly as the number of methylene spacer groups in PI-*n*CN increases (see Table 1). In a previous paper,[7] Kim and Han reported a very strong molecular weight dependence of η and N_1 of segmented MCLCPs ($\eta \propto M^6$ and $N_1 \propto M^{6.7}$). At present, we do not have information on the molecular weight dependence of η and N_1 of SCLCPs. Intuitively, we would expect that the molecular weight dependence of η and N_1 of SCLCPs would be weaker than that of MCLCPs and that it would depend on the flexible spacer length of SCLCPs. The reason is that the longer the flexible spacer of SCLCP, the greater will be decoupling between the side-chain liquid-crystalline monomers and the polymer backbone. Using this argument, we can now explain why in Figure 7 the values of η and N_1 of PI-11CN are smaller than those of PI-7CN and PI-5CN, and the values of η and N_1 of PI-7CN are smaller than those of PI-5CN. In other words, the contributions of side-chain liquid-crystalline monomers to the η and N_1 of PI-*n*CN become smaller as the number of flexible spacer groups increases from 5 to 11.

Temperature Dependence of Steady-State Shear Viscosity. Figure 8 describes variations of η with temperature for (a) PI-5CN, (b) PI-7CN, and (c) PI-11CN, which were obtained from temperature sweep experiments in steady-state shear mode at $\dot{\gamma} = 1.0\ s^{-1}$. In obtaining the results, the temperature was increased stepwise at a rate of 1 °C/min from an anisotropic region (at $T < T_{cl}$) to the isotropic state (at $T > T_{cl}$). To facilitate our discussion, also given in Figure 8 are DSC traces for all three PI-*n*CNs. It is seen in Figure 8a that the η of PI-5CN decreases monotonically with increasing temperature from 75 °C, passing through T_{cl} (102 °C), to 130 °C. This temperature dependence of η for PI-5CN is quite different from that for nematic-forming MCLCPs reported previously by Han and co-workers.[8,69] Specifically, they made the following observations: the η in the nematic region first decreased with increasing temperature, going through a minimum, then increased going through a maximum as the temperature approached T_{cl}, and finally decreased steadily with a further increase in temperature in the isotropic region. They attributed the decreasing trend of η in the nematic region with increasing temperature to an enhanced orientation of the liquid crystalline phase and attributed

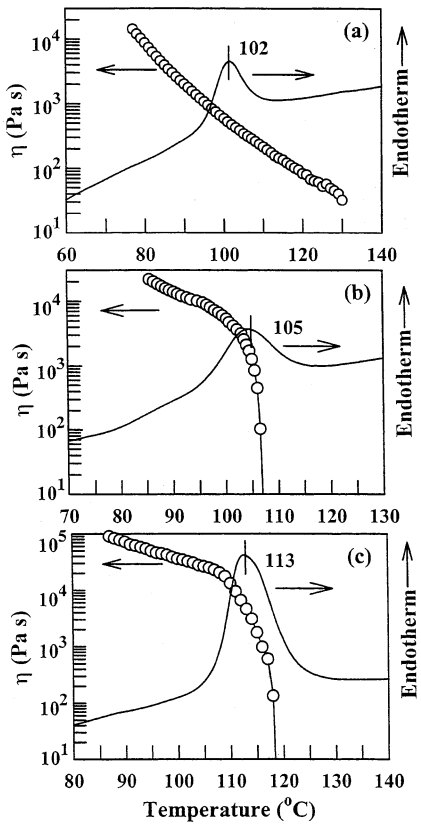

Figure 8. Variations of η with temperature for (a) PI-5CN, (b) PI-7CN, and (c) PI-11CN at $\dot{\gamma} = 0.1\ s^{-1}$. The solid line is a DSC trace obtained at a heating rate of 20 °C/min.

the increasing trend of η before reaching T_{cl} to the formation of isotropic phase. Thus, we tentatively conclude that the steady decrease of η for PI-5CN with increasing temperature, given in Figure 8a, is not due to the orientation of nematic mesophase under shear flow, which was the case for segmented MCLCPs,[8,69] but rather due to the steady loss of the strength of nematics in PI-5CN with increasing temperature.

We can use the above argument to explain the temperature dependence of η for PI-7CN given in Figure 8b and for PI-11N given in Figure 8c, in which we observe that in the anisotropic region the η of PI-7CN and PI-11CN decreases steadily until reaching T_{cl}, at which the η drops precipitously, signifying a first-order transition. The temperature dependence of η for PI-7CN and PI-11CN shown in Figure 8b,c looks very similar to the temperature dependence of dynamic storage modulus (G') of lamella- or cylinder-forming block copolymers during isochronal dynamic temperature sweep experiments in that values of G' drop precipitously at T_{ODT}. In the past, numerous research groups determined the T_{ODT} of cylinder- and lamella-forming block copolymers from isochronal dynamic temperature sweep experiments. There are too many papers to cite them all here, and therefore the readers are referred to the seminal paper of Gouinlock and Porter[94] and a paper by Han and co-workers.[95] The temperature dependence of η for PI-7CN given in Figure 8b and for PI-11CN given in Figure 8c suggests that the side-chain liquid-crystalline monomers and the polymer backbone are very much decoupled to the extent that the η of PI-7CN or PI-11CN is determined very much by the η of the polymer backbone once the side-chain liquid-crystalline monomers undergo isotropization at T_{cl}. Note that the

molecular weights of the polymer backbone PI in PI-7CN and PI-11CN are fairly low (see Table 1), and thus the η of the polymer backbone at $T > 100$ °C is expected to be very low.

It seems appropriate to mention at this juncture that the temperature dependence of η for PI-5CN given in Figure 8a resembles very much the one reported earlier by Colby et al.,[55] who also employed a nematic-forming SCLCP. Ostensibly, the temperature dependence of η for PI-5CN (see Figure 8a) resembles very much the temperature dependence of η often observed in ordinary flexible polymers. Thus, one may be tempted to conclude that the rheological behavior of SCLCPs in general is very similar to that of ordinary flexible polymers. But it is clear from Figure 8b for PI-7CN and from Figure 8c for PI-11CN that the rheological behavior of SCLCPs in general cannot be regarded as being very similar to that of ordinary flexible polymers. The differences in the rheological behavior between SCLCPs and ordinary flexible polymers will become clearer when we present below the responses to initial start-up transient shear flow and intermittent transient shear flow of PI-*n*CNs.

Transient Shear Flow without Preshearing. In this study we investigated transient shear flow of PI-5CN, PI-7CN, and PI-11CN which had the following thermal histories. A specimen was first placed in the cone-and-plate fixture that was preheated about 20 °C above the T_{cl} of each polymer specimen. After the temperature of the specimen was equilibrated in the isotropic region, it was cooled to a predetermined temperature in the anisotropic region, and the specimen was allowed to reach thermal equilibrium for about 0.5−4 h. This procedure resulted in a reproducible initial condition. Figure 9 describes the evolution of first normal stress difference growth $N_1^+(\dot{\gamma},t)$ as a function of applied strain ($\dot{\gamma}t$), and Figure 10 describes the evolution of shear stress growth $\sigma^+(\dot{\gamma},t)$ as a function of applied ($\dot{\gamma}t$) for (a) PI-5CN at 70 °C, (b) PI-7CN at 75 °C, and (c) PI-11CN at 90 °C upon start-up of shear flow at $\dot{\gamma} = 1.0\ s^{-1}$ and $T_{cl} - T \approx 25-30$ °C. The following observations are worth noting in Figures 9 and 10. In Figure 9 we observe that PI-5CN and PI-7CN exhibit large overshoot peaks of $N_1^+(\dot{\gamma},t)$, while PI-11CN exhibits a smaller overshoot peak of $N_1^+(\dot{\gamma},t)$. A similar observation can be made on the overshoot peaks of $\sigma^+(\dot{\gamma},t)$ in Figure 10. The magnitude of $N_1^+(\dot{\gamma},t)$ and $\sigma^+(\dot{\gamma},t)$ decreases as the number of methylene spacer groups increases from 5 to 11. Specifically, values of $N_1^+(\dot{\gamma},t)$ and $\sigma^+(\dot{\gamma},t)$ for PI-7CN are approximately one-half of those for PI-5CN, and the values of $N_1^+(\dot{\gamma},t)$ and $\sigma^+(\dot{\gamma},t)$ for PI-11CN are less than one-tenth of those for PI-5CN. In preparing Figures 9 and 10, we used measured values of $N_1^+(\dot{\gamma},t)$ and $\sigma^+(\dot{\gamma},t)$, instead of normalized quantities $N_1^+(\dot{\gamma},t)/N_1$ and $\sigma^+(\dot{\gamma},t)/\sigma$ in order to show how the magnitudes of $N_1^+(\dot{\gamma},t)$ and $\sigma^+(\dot{\gamma},t)$ decrease with increasing flexible spacer length. We attribute such large differences in the magnitude of $N_1^+(\dot{\gamma},t)$ and $\sigma^+(\dot{\gamma},t)$ among the three PI-*n*CNs to stronger decoupling as the number of methylene spacer groups increases from 5 to 11. Nevertheless, the ratio of the overshoot peak value $N_1^+(\dot{\gamma},t)$ and steady-state value N_1, $N_{1,peak}^+(\dot{\gamma},t)/N_1$, does not change as dramatically as $N_1^+(\dot{\gamma},t)$ itself: $N_{1,peak}^+(\dot{\gamma},t)/N_1 = 1.95$ for PI-5CN, 1.85 for PI-7CN, and 1.61 for PI-11CN as the number of methylene spacer groups increases from 5 to 11.

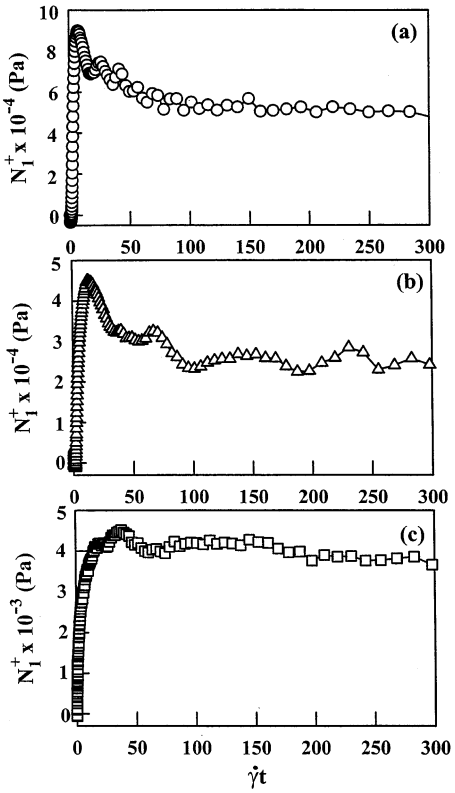

Figure 9. Variations of $N_1^+(\dot{\gamma},t)$ with $\dot{\gamma}t$ upon start-up of shear flow at $\dot{\gamma} = 1.0\ s^{-1}$ for specimens without preshearing: (a) PI-5CN at 70 °C, (b) PI-7CN at 75 °C, and (c) PI-11CN at 90 °C. The thermal histories of the specimens are as follows. Each specimen was first placed in the cone-and-plate fixture that was preheated to a temperature about 20 °C above its T_{cl} in the isotropic region. After the temperature of the specimen was equilibrated in the isotropic region, it was cooled to a temperature about 25−30 °C below its T_{cl} in the anisotropic region, and the specimen was allowed to reach thermal equilibrium for 0.5−4 h before being subjected to start-up of shear flow.

In Figures 9 and 10, we observe little differences in the liquid-crystalline characteristics of transient shear responses among the three PI-*n*CNs, very similar to that observed in MCLCPs.[4−7,9−12] On the other hand, in Figure 7 we have already observed that PI-5CN exhibits the shear rate dependence of steady-state viscosity very similar to that of high-molecular-weight ordinary flexible polymers, while PI-7CN and PI-11CN exhibit strong shear-thinning behavior over the entire range of shear rates tested. It is well-established today that high-molecular-weight ordinary flexible polymers do not exhibit large stress overshoots during transient shear flow. Thus, we conclude that transient shear flow responses are much more sensitive to the differences in the morphological state of polymers (e.g., SCLCP vs ordinary flexible polymers) than steady-state shear flow responses, and thus the rheological behavior of PI-5CN should not be regarded as being similar to that of ordinary flexible polymers solely on the basis of steady-state shear responses.

A question then remains to be answered: What is the origin of large stress overshoots observed in Figures 9 and 10 for PI-5CN? We attribute the origin of large stress overshoots observed for PI-5CN (also in PI-7CN and PI-11CN) to the reorientation, upon start-up of shear flow, of initially, randomly oriented domains toward the flow direction, advocated for MCLCPs by Ugaz et al.[96] Our view is based on the structural

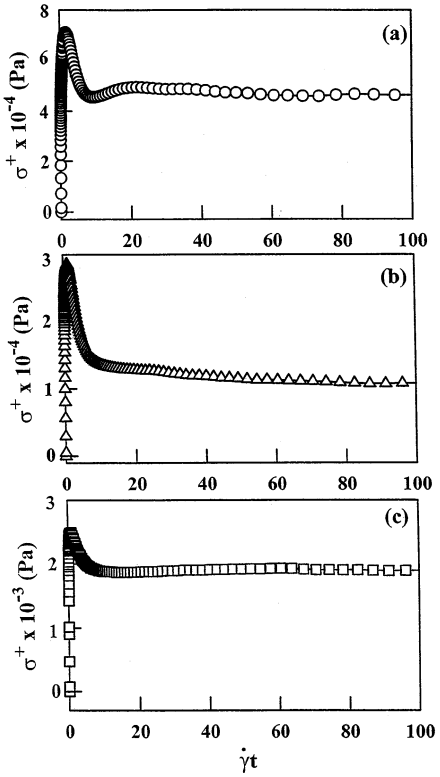

Figure 10. Variations of $\sigma^+(\dot{\gamma},t)$ with $\dot{\gamma}t$ upon start-up of shear flow at $\dot{\gamma} = 1.0$ s^{-1} for specimens without preshearing: (a) PI-5CN at 70 °C, (b) PI-7CN at 75 °C, and (c) PI-11CN at 90 °C. The thermal histories of the specimens are the same as described in the caption of Figure 9.

consideration: the nematic mesophase in PI-5CN and the smectic mesophase in PI-7CN and PI-11CN. Specifically, the forces required for reorienting the initially, randomly oriented domains in PI-5CN, for instance, toward the flow direction would be much greater than the forces required for reorienting high-molecular-weight ordinary flexible polymers. Once steady state is reached, the steady-state shear responses of PI-5CN may be little different from those of high-molecular-weight ordinary flexible polymers.

We surmise that the influence of the nematic mesophase in SCLCPs on steady-state shear responses would be much weaker, owing to decoupling between the side-chain liquid-crystalline monomers and the polymer backbone, than the influence of the nematic mesophase in MCLCPs in which the nematic mesophase is part of the entire polymer chain. The situation is expected to be quite different for the smectic-forming PI-7CN and PI-11CN because these two polymers have layered structures of smectic mesogenics. Specifically, the reorientation of the initially, randomly oriented domains in the smectic-forming PI-7CN and PI-11CN, upon start-up of shear flow, toward the flow direction would require much greater forces than that in the nematic-forming PI-5CN. This is probably the reason why the steady-state shear viscosities of smectic-forming PI-7CN and PI-11CN exhibit strong shear-thinning behavior at low shear rates (Figure 7).

Transient Shear Flow with Presheared and Squeezed Specimens. In this study we also conducted transient shear flow experiments using our SCLCP specimens after they were presheared and then squeezed before start-up shear flow was applied. The experiments were motivated by the previous studies of Quijada-Garrido et al.,[62,63] who reported on sustained, regular oscillations of $N_1^+(\dot{\gamma},t)$ during transient shear flow of their SCLCP specimens that were presheared and then squeezed. In our study we have tried to duplicate the thermal and deformation histories of specimens described in a paper of Quijada-Garrido et al.[62] Specifically, the following experimental protocol was employed in our experiment. A specimen of PI-11CN was first loaded into the cone-and-plate fixture preheated to a temperature (T_{cl} + 20 °C) in the isotropic region, and the gap opening of the cone-and-plate fixture was adjusted to 70 μm. After reaching thermal equilibrium in the isotropic region, the specimen was cooled slowly to a predetermined temperature ($T_{cl} - T = 20$ °C) in the anisotropic region. During cooling, the gap opening of the cone-and-plate fixture was maintained at 70 μm by compensating for the changes in the thermal contraction of the metal. After waiting for 4 h to attain thermal equilibrium in the anisotropic region, the specimen was presheared at a shear rate ($\dot{\gamma}$) of 0.3 s^{-1} for 20 min followed by squeezing of the gap opening to 50 μm.

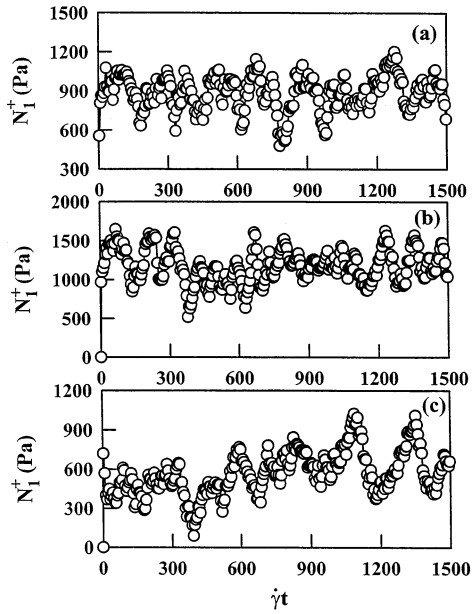

Figure 11. (a) Variations of $N_1^+(\dot{\gamma},t)$ for a PI-11CN specimen, which was presheared and squeezed in the anisotropic state at 90 °C, with applied $\dot{\gamma}t$ upon start-up of shear flow at $\dot{\gamma} = 0.7$ s^{-1}. (b) Variations of $N_1^+(\dot{\gamma},t)$ with applied $\dot{\gamma}t$ after the stepping-up of shear rate from 0.7 to 1.0 s^{-1}. (c) Variations of $N_1^+(\dot{\gamma},t)$ with applied $\dot{\gamma}t$ after the stepping-down of shear rate from 1.0 to 0.5 s^{-1}. The thermal histories of the specimens are as follows. The specimen was placed in the cone-and-plate fixture that was preheated to a temperature about 20 °C above its T_{cl} in the isotropic region, and the gap opening was adjusted to 70 μm. After the specimen reached thermal equilibrium, it was cooled slowly to a temperature about 20 °C below its T_{cl} in the anisotropic region. After the specimen reached thermal equilibrium, it was presheared at T_{cl} for 20 min and then squeezed to 50 μm of gap opening.

After squeezing the specimen, start-up of shear flow was applied at $\dot{\gamma} = 0.7$ s^{-1} and shearing continued for 30 min. Figure 11a describes the evolution of first normal stress difference $N_1^+(\dot{\gamma},t)$ for PI-11CN at 90 °C as a function of applied $\dot{\gamma}t$ for 1500 strain units during the initial transient shear flow, showing that the oscillatory behavior in $N_1^+(\dot{\gamma},t)$ is not regular. After shearing of the specimen at $\dot{\gamma} = 0.7$ s^{-1} for 1500 strain units, the shear rate was increased rapidly to 1.0 s^{-1}

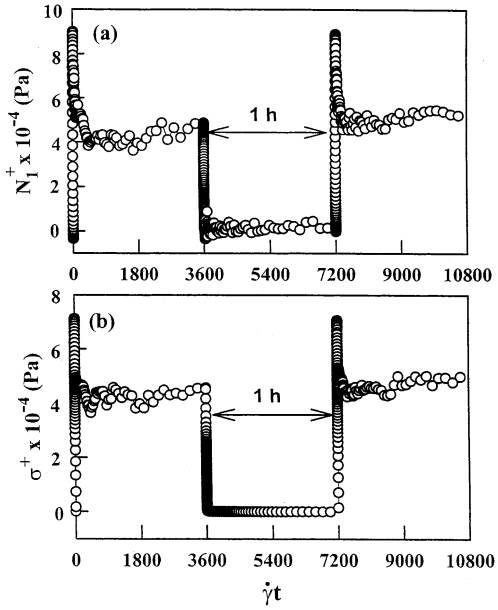

Figure 12. (a) Variations of $N_1^+(\dot{\gamma},t)$ with $\dot{\gamma}t$ and (b) variations of $\sigma^+(\dot{\gamma},t)$ with $\dot{\gamma}t$ for PI-5CN at 70 °C in the nematic region during the initial start-up transient at $\dot{\gamma} = 1.0$ s^{-1} for 1 h followed by a rest for 1 h and during the intermittent transient at $\dot{\gamma} = 1.0$ s^{-1} for 1 h. The thermal history of the specimen is the same as described in the caption of Figure 9.

(i.e., a step-up of shear rate). Figure 11b describes the evolution of $N_1^+(\dot{\gamma},t)$ as a function of applied $\dot{\gamma}t$ for 1500 strain units after the step-up of shear rate from 0.7 to 1.0 s^{-1}, showing again that the oscillatory behavior in $N_1^+(\dot{\gamma},t)$ is not regular. After shearing of the specimen at $\dot{\gamma} = 1.0$ s^{-1} for 1500 strain units, the shear rate was decreased rapidly to 0.5 s^{-1} (i.e., a step-down of shear rate). Figure 11c describes the evolution of $N_1^+(\dot{\gamma},t)$ as a function of applied $\dot{\gamma}t$ for 1500 stain units after the step-down of shear rate from 1.0 to 0.5 s^{-1}, showing that the oscillatory behavior in $N_1^+(\dot{\gamma},t)$ has become more irregular. Similar experiments were performed at different temperatures in the anisotropic region and also at different shear rates. Our experimental results presented in Figure 11 stand in contrast with the findings reported earlier by Quijada-Garrido et al.[62,63] In all of our experiments of transient shear flow with preshearing and squeezing of a specimen, we were not able to obtain reproducible results. At present we cannot explain the origin of the irregular oscillatory behavior of $N_1^+(\dot{\gamma},t)$ observed in Figure 11, which does not seem to conform with the expectation of director tumbling.[62,63]

Intermittent Shear Flow. In the past, intermittent shear flow of MCLCPs has been investigated.[12,97,98] In the present study we conducted intermittent shear flow experiments for PI-5CN, PI-7CN, and PI-11CN. In so doing, we varied the duration of rest upon cessation of steady shear flow before applying another transient shear flow. Figure 12 describes the evolution of $N_1^+(\dot{\gamma},t)$ and $\sigma^+(\dot{\gamma},t)$ as a function of applied $\dot{\gamma}t$ in PI-5CN at 70 °C in the nematic region during the initial start-up transient flow for 1 h at $\dot{\gamma} = 1.0$ s^{-1}, followed by a rest for 1 h upon cessation of shear flow, and during the intermittent transient flow for 1 h at $\dot{\gamma} = 1.0$ s^{-1}. In Figure 12, we observe that PI-5CN exhibits large overshoot peaks of $N_1^+(\dot{\gamma},t)$ and $\sigma^+(\dot{\gamma},t)$ during the intermittent transient flow, the magnitudes of which are virtually the same as those during the initial start-up

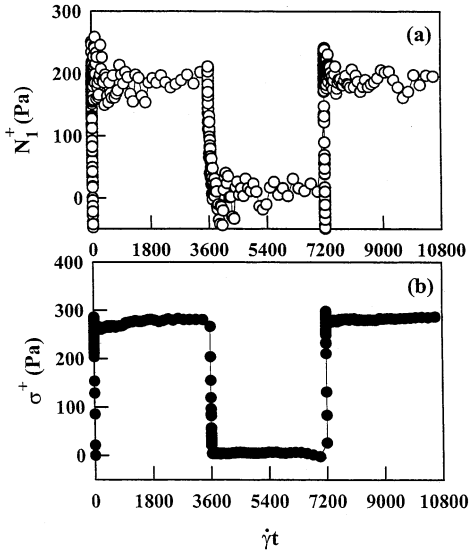

Figure 13. (a) Variations of $N_1^+(\dot{\gamma},t)$ with $\dot{\gamma}t$ and (b) variations of $\sigma^+(\dot{\gamma},t)$ for PI-5CN at 110 °C in the isotropic region during the initial start-up transient at $\dot{\gamma} = 1.0$ s^{-1} for 1 h, followed by a rest for 1 h, and during the intermittent transient at $\dot{\gamma} = 1.0$ s^{-1} for 1 h.

transient flow. This observation suggests that structural reorganization in PI-5CN has been completed after a rest for 1 h upon cessation of shear flow.

Figure 13 describes the evolution of $N_1^+(\dot{\gamma},t)$ and $\sigma^+(\dot{\gamma},t)$ as a function of applied $\dot{\gamma}t$ in PI-5CN at 110 °C in the isotropic region during the initial start-up transient flow for 1 h at $\dot{\gamma} = 1.0$ s^{-1}, followed by a rest for 1 h upon cessation of shear flow, and during the intermittent transient flow for 1 h at $\dot{\gamma} = 1.0$ s^{-1}. In Figure 13, we observe small overshoot peaks in both $N_1^+(\dot{\gamma},t)$ and $\sigma^+(\dot{\gamma},t)$ in the isotropic phase of PI-5CN, compared to those in the nematic region given in Figure 12. There is no resemblance in the nonlinear transient flow of PI-5CN between the isotropic and nematic phases, and values of both $N_1^+(\dot{\gamma},t)$ and $\sigma^+(\dot{\gamma},t)$ in the nematic phase are 2 orders of magnitude greater than those in the isotropic phase. Such a dramatic difference in transient shear responses between the nematic and isotropic phases has also been observed in MCLCPs.[4−7,9−12]

In this study, using a high-molecular-weight polyisoprene (PI-270) having $M_w = 2.7 \times 10^5$ we also conducted transient shear flow experiment to compare with the transient shear responses of PI-5CN in the nematic phase. Here we chose homopolymer PI because our SCLCPs investigated in this study, PI-*n*CNs, are based on a PI backbone. Figure 14 describes the evolution of $N_1^+(\dot{\gamma},t)$ and $\sigma^+(\dot{\gamma},t)$ as a function of applied $\dot{\gamma}t$ in PI-270 at 200 °C during the initial start-up transient flow for 10 min at $\dot{\gamma} = 1.0$ s^{-1}, followed by a rest for 10 min upon cessation of shear flow, and during the intermittent transient flow for 10 min at $\dot{\gamma} = 1.0$ s^{-1}. Notice in Figure 14 that there is virtually no overshoot of $N_1^+(\dot{\gamma},t)$ and $\sigma^+(\dot{\gamma},t)$ in PI-270 during both the initial start-up transient flow and the intermittent transient flow. Comparison of Figure 14 with Figure 12 reveals very clearly that there is no resemblance whatsoever in the nonlinear transient flow between the nematic-forming PI-5CN and high-molecular-weight ordinary flexible polymer PI-270. Therefore, we conclude that the nonlinear transient flow of PI-5CN given in Figure 12 is attributable solely to the presence of liquid crystallinity in PI-5CN.

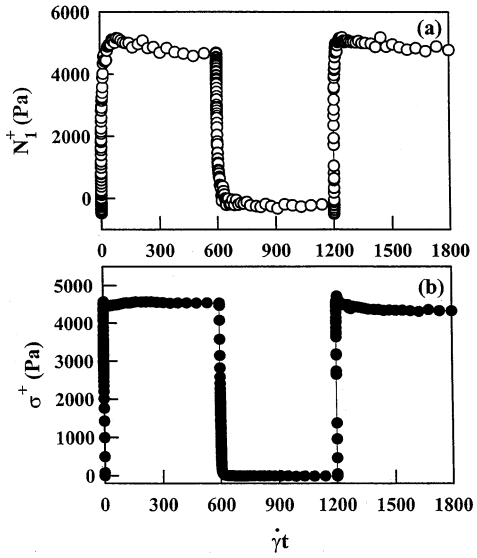

Figure 14. (a) Variations of $N_1^+(\dot{\gamma},t)$ with $\dot{\gamma}t$ and (b) variations of $\sigma^+(\dot{\gamma},t)$ with $\dot{\gamma}t$ for PI-270 at 200 °C during the initial start-up transient at $\dot{\gamma} = 1.0$ s^{-1} for 10 min, followed by a rest for 10 min, and during the intermittent transient at $\dot{\gamma} = 1.0$ s^{-1} for 10 min.

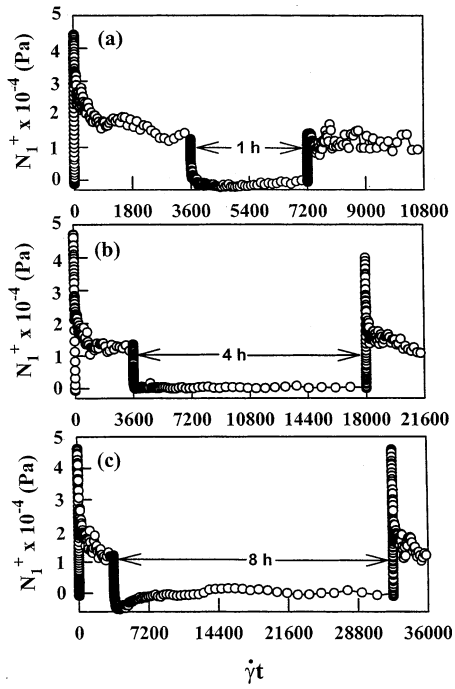

Figure 15. Variations of $N_1^+(\dot{\gamma},t)$ with $\dot{\gamma}t$ for PI-7CN at 75 °C: (a) during the start-up transient at $\dot{\gamma} = 1.0$ s^{-1}, followed by a rest for 1 h, and during the intermittent transient at $\dot{\gamma} = 1.0$ s^{-1}; (b) during the start-up transient at $\dot{\gamma} = 1.0$ s^{-1}, followed by a rest for 4 h, and during the intermittent transient at $\dot{\gamma} = 1.0$ s^{-1}; (c) during the start-up transient at $\dot{\gamma} = 1.0$ s^{-1}, followed by a rest for 8 h, and during the intermittent transient at $\dot{\gamma} = 1.0$ s^{-1}. The thermal history of the specimen is the same as described in the caption of Figure 9.

Figure 15a describes the evolution of $N_1^+(\dot{\gamma},t)$ as a function of applied $\dot{\gamma}t$ in PI-7CN at 75 °C in the smectic region during the initial start-up transient flow for 1 h at $\dot{\gamma} = 1.0$ s^{-1}, followed by a rest for 1 h upon cessation of shear flow, and during the intermittent transient flow for 1 h at $\dot{\gamma} = 1.0$ s^{-1}. In Figure 15a, we observe that the overshoot peak of $N_1^+(\dot{\gamma},t)$ during the intermittent transient flow after a rest for 1 h upon cessation of shear flow is very small compared to that during the initial start-up transient flow. This observation suggests that a rest for 1 h upon cessation of shear flow was too short for PI-7CN to have measurable structural reorganization in $N_1^+(\dot{\gamma},t)$. After a rest for 4 h upon cessation of the initial start-up transient flow, in Figure 15b we observe that the overshoot peak of $N_1^+(\dot{\gamma},t)$ during the intermittent transient flow is about 90% of that observed during the initial start-up transient flow, suggesting that substantial structural reorganization in $N_1^+(\dot{\gamma},t)$ took place during a rest for 4 h. After a rest for 8 h upon cessation of the initial start-up transient flow, in Figure 15c we observe that virtually complete structural reorganization in $N_1^+(\dot{\gamma},t)$ has taken place in that the overshoot peak of $N_1^+(\dot{\gamma},t)$ during the intermittent transient flow is virtually identical to that in the initial start-up transient flow. Comparison of Figure 15 with Figure 12 indicates that PI-7CN having seven methylene spacer groups requires, upon cessation of shear flow, much longer time for structural reorganization in $N_1^+(\dot{\gamma},t)$ compared to PI-5CN having five methylene spacer groups. However, the observed difference in structural reorganization in $N_1^+(\dot{\gamma},t)$ between PI-7CN and PI-5CN is not solely due to the difference in flexible spacer length because PI-7CN has smectic mesophase while PI-5CN has nematic mesophase (see Figure 3). Longer time required for structural reorganization, upon cessation of shear flow, for PI-7CN can be understood when we recognize the fact that PI-7CN has two-dimensional layered structure of smectic mesophase, while PI-5CN has one-dimensional nematic mesophase. We have found that the overshoot peak of $\sigma^+(\dot{\gamma},t)$ observed during the initial transient flow, although it is not presented here, was recovered during the intermittent transient flow after a rest of ca. 4 h, indicating that structural reorganization in $\sigma^+(\dot{\gamma},t)$ is much faster than that in $N_1^+(\dot{\gamma},t)$.

Figure 16 describes the evolution of $N_1^+(\dot{\gamma},t)$ as a function of applied $\dot{\gamma}t$ in PI-11CN at 90 °C in the smectic region during the initial start-up transient flow for 1 h at $\dot{\gamma} = 1.0$ s^{-1}, followed by a rest for 4, 8, or 12 h upon cessation of shear flow, and during the intermittent transient flow for 1 h at $\dot{\gamma} = 1.0$ s^{-1}. In Figure 16a, we observe that the overshoot peak of $N_1^+(\dot{\gamma},t)$ during the intermittent transient flow after a rest for 4 h upon cessation of shear flow is about 67% of that observed during the initial start-up transient flow. After a rest for 8 h upon cessation of the initial start-up transient flow, in Figure 16b we observe that structural reorganization in $N_1^+(\dot{\gamma},t)$ has achieved about 93%. After a rest for 12 h upon cessation of the initial start-up transient flow, in Figure 16c we observe that virtually complete structural reorganization in $N_1^+(\dot{\gamma},t)$ has taken place in that the overshoot peak of $N_1^+(\dot{\gamma},t)$ during the intermittent transient flow is virtually identical to that in the initial start-up transient flow. Comparison of Figure 16 with Figure 15 indicates that PI-11CN having 11 methylene spacer groups requires, upon cessation of shear flow, much longer time for structural reorganization in $N_1^+(\dot{\gamma},t)$ compared to PI-7CN having seven methylene spacer groups. Since both PI-11CN and PI-7CN have smectic mesophase, we attribute the above observation to the difference in flexible spacer length between PI-11CN and PI-7CN. We have found that that the overshoot peak of $\sigma^+(\dot{\gamma},t)$ observed during the initial transient shear flow, al-

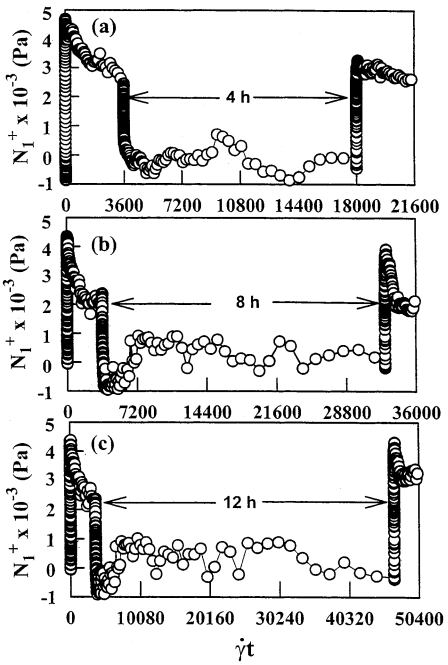

Figure 16. Variations of $N_1^+(\dot{\gamma},t)$ with $\dot{\gamma}t$ for PI-11CN at 90 °C: (a) during the start-up transient at $\dot{\gamma} = 1.0\ s^{-1}$, followed by a rest for 4 h, and during the intermittent transient at $\dot{\gamma} = 1.0\ s^{-1}$; (b) during the start-up transient at $\dot{\gamma} = 1.0\ s^{-1}$, followed by a rest for 8 h, and during the intermittent transient at $\dot{\gamma} = 1.0\ s^{-1}$; (c) during the start-up transient at $\dot{\gamma} = 1.0\ s^{-1}$, followed by a rest for 12 h, and during the intermittent transient at $\dot{\gamma} = 1.0\ s^{-1}$. The thermal history of the specimen is the same as described in the caption of Figure 9.

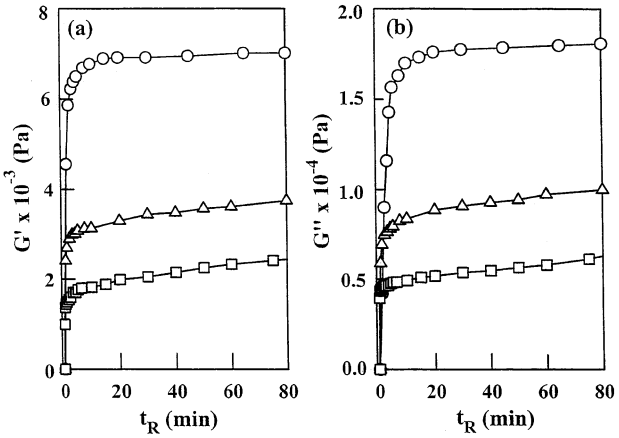

Figure 17. (a) Time evolution of dynamic storage modulus G' and (b) time evolution of dynamic loss modulus G'' upon cessation of steady shear flow at $\dot{\gamma} = 1.0\ s^{-1}$, which were monitored at an angular frequency of 1.0 rad/s for (○) PI-5CN, (△) PI-7CN, and (□) PI-11CN.

though it is not presented here, was recovered during the intermittent transient flow after a rest of ca. 8 h, indicating that structural reorganization in $\sigma^+(\dot{\gamma},t)$ is much faster than that in $N_1^+(\dot{\gamma},t)$.

Time Evolution of Dynamic Moduli after Cessation of Shear Flow. In the present study we monitored time evolution of G' and G'' upon cessation of shear flow by applying small-amplitude oscillatory deformation to the specimen. Figure 17a describes the evolution of G', and Figure 17b describes the evolution of G'', as a function of rest period (t_R) upon cessation of shear flow of PI-5CN at 90 °C, PI-7CN at 95 °C, and PI-11CN at 100 °C, after each specimen had been sheared in steady-state mode at $\dot{\gamma} = 1.0\ s^{-1}$ for 1 h. It is seen in Figure 17 that values of G' and G'' for PI-5CN initially increase very rapidly and then slowly to reach a constant value about 20 min after cessation of shear flow, while values of G' and G'' for PI-7CN and PI-11CN do not attain a constant value even after 80 min upon cessation of steady shear flow. Specifically, a longer rest period upon cessation of steady shear flow is required as the number of methylene spacer groups in PI-*n*CN increases from 5 to 11. The readers are reminded that PI-5CN has a nematic mesophase, while PI-7CN and PI-11CN have a smectic mesophase (see Figure 3). Earlier, a similar observation was made by Wewerka et al.[64] An increase in G' upon cessation of shear flow may be viewed as signifying a recovery of the deformed domain texture (i.e., structural reorganization takes place) after shear flow stops. The experimental results summarized in Figure 17 suggest that very slow structural reorganization takes place in the smectic-forming PI-7CN and PI-11CN than in the nematic-forming PI-5CN. Thus, we can conclude that the number of methylene spacer groups in PI-*n*CNs (thus flexible spacer length in SCLCPs in general) has a profound influence on the rate of structural reorganization upon cessation of steady shear flow.

Banded Structure of SCLCP. In the 1980s and 1990s, a number of research groups[99−106] reported on the formation of banded structure of MCLCPs, but very few investigators reported on the formation of banded structure of SCLCPs. The paucity of the literature reporting on the experimental observation of banded structure of SCLCP is, apparently, due to the relatively flexible nature of SCLCPs as compared to the more rigid MCLCPs. In 1998, Tang et al.[107] reported on their observation of the banded structure of an SCLCP (PA8CN), which had polyacetylene as the polymer backbone and 8CN-COOH as the side-chain liquid-crystalline monomer. In the present study we observed banded structure from our SCLCPs, and Figure 18 gives an image of the banded structure of a thin PI-11CN film observed under a polarized optical microscope at 95 °C. The banded structure shown in Figure 18 was generated by mechanical shearing of a PI-11CN specimen placed between two glass plates preheated to 95 °C, which is about 20 °C below the clearing temperature of PI-11CN.

4. Concluding Remarks

In this study we have investigated rheological behavior of model SCLCPs that were synthesized by grafting a liquid-crystalline monomer, [*n*-[(4-cyanobiphenyl)oxy]-alkyl]carboxylic acid (*n*CN-COOH) with varying number of methylene groups (n = 5, 7, or 11), onto a nearly monodisperse hydroxylated polyisoprene, yielding poly-{[*n*-[(4-cyanobiphenyl)oxy]alkyl]carbonyl}oxyisoprenes (PI-*n*CN). The PI-*n*CN employed for our rheological investigation were nearly monodisperse, having a polydispersity index less than 1.1, because the polymer backbone PI of the SCLCPs was first synthesized using anionic polymerization, yielding nearly monodisperse polymer, followed by hydroxylation. The use of the nearly monodisperse SCLCPs synthesized in this study gave us advantages in interpreting our rheological data over polydisperse SCLCPs often obtained by condensation polymerization that invariably gives rise to a high polydispersity index. We synthesized PI-*n*CNs with three different methylene spacer groups: PI-5CN, PI-7CN, and PI-11CN. Using these polymers, we investigated the effect of flexible spacer length on the rheo-

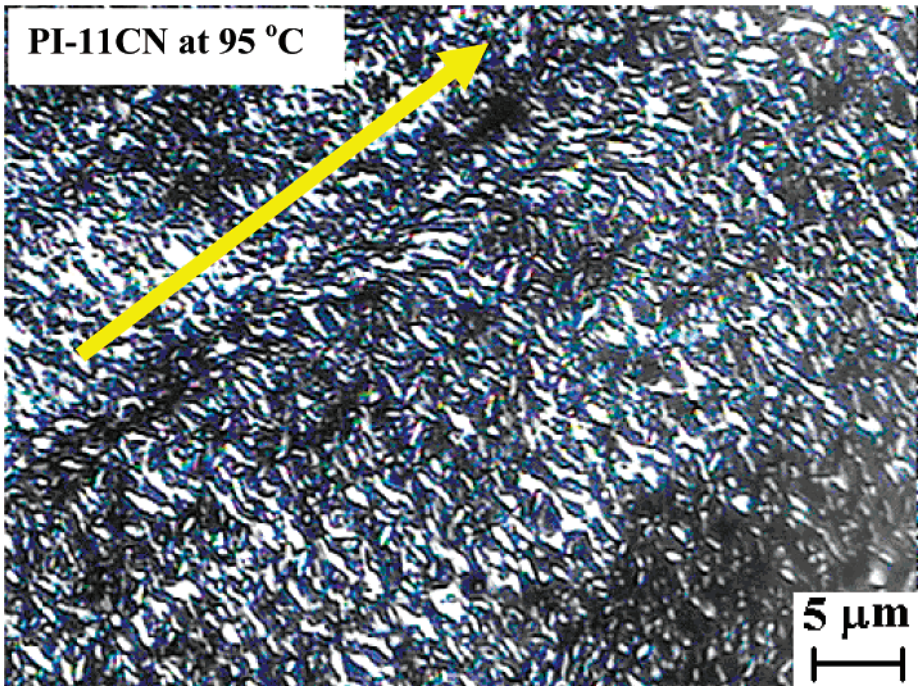

Figure 18. Banded structure of a thin PI-11CN film after being subjected to mechanical shearing at 95 °C, in which the arrow indicates the direction of shear.

logical behavior of SCLCPs. The highlights of our findings are as follows.

We have observed different liquid-crystalline states in PI-*n*CN, depending upon the flexible spacer length, specifically PI-5CN having a nematic mesophase and PI-7CN and PI-11CN having a smectic mesophase. Such an experimental observation is found to be in general agreement with the previous studies reported in the literature,[42,45,64] namely SCLCPs having short spacer length tend to have a nematic mesophase and SCLCPs having long spacer length tend to have a smectic mesophase.

We have observed large overshoot peaks in transient stresses, $N_1^+(\dot{\gamma},t)$ and $\sigma^+(\dot{\gamma},t)$ in PI-*n*CN upon start-up of shear flow, that distinguish SCLCPs from ordinary flexible polymers. We have observed that the magnitude of viscosity (η) and first normal stress difference (N_1) in steady-state shear flow decreases as the number (n) of methylene spacer groups in PI-*n*CN increases from 5 to 7 and to 11 (Figure 7) and also the magnitude of $N_1^+(\dot{\gamma},t)$ and $\sigma^+(\dot{\gamma},t)$ in PI-*n*CN during transient shear flow decreases as the number of methylene spacer groups in PI-*n*CN increases from 5 to 7 and to 11 (Figures 9 and 10). The decrease in η and N_1 and also the decrease in $N_1^+(\dot{\gamma},t)$ and $\sigma^+(\dot{\gamma},t)$ with increasing flexible spacer length are attributable to an enhanced decoupling between the polymer backbone and side-chain LC monomer as the flexible spacer length in PI-*n*CN increases. According to Craig and Imrie,[42] cyanobiphenyl-based SCLCPs generally form partially interdigitated smectic phase, in which the backbone lies between the smectic layers. As the flexible spacer length increases, the backbones may be considered to be largely unaffected by the smectic mesogenics and thus reside in an essentially isotropic conformation.

We have also observed that the structural reorganization upon cessation of shear flow is much slower in the smectic-forming PI-7CN and PI-11CN than in the nematic-forming PI-5CN. The experimental observations indicate that the type of order and the length scale of the mesogenic unit have a profound influence on the rheological behavior of PI-*n*CNs. As the flexible spacer length (n) in PI-*n*CN increases, decoupling of the mesogenic unit from the polymer backbone increases and thus the arrangement of the side-chain LC monomers becomes increasingly important to the rheological behavior of SCLCPs. Specifically, the degree of packing of the layered structure would play a central role in determining the rheological responses of SCLCPs.

We have observed large differences in the evolution of $N_1^+(\dot{\gamma},t)$ and $\sigma^+(\dot{\gamma},t)$ with applied $\dot{\gamma}t$ during transient shear flow between the nematic-forming PI-5CN and ordinary flexible polymers, while the shear rate dependence of η and N_1 in steady-state shear flow for PI-5CN looks similar to that for ordinary flexible polymers. Thus, we have concluded that transient shear flow is much more sensitive than steady-state shear flow in distinguishing the rheological behavior of PI-5CN from that of ordinary flexible polymers.

Acknowledgment. We acknowledge that this study was supported in part by the National Science Foundation under Grant CTS-9981972.

References and Notes

(1) Wissbrun, K. F.; Griffin, A. C. *J. Polym. Sci., Polym. Phys. Ed.* **1982**, *20*, 1835.
(2) Wunder, S. L.; Ramachandran, S.; Cochanour, C. R.; Weinberg, M. *Macromolecules* **1986**, *19*, 1696.
(3) Irwin, R. S.; Sweeny, W.; Gardner, K. H.; Gochanour, C. R.; Weinberg, M. *Macromolecules* **1989**, *22*, 1065.
(4) Cocchini, F.; Nobile, M. R.; Acierno, D. *J. Rheol.* **1991**, *35*, 1171.
(5) Driscoll, P.; Masuda, T.; Fujiwara, K. *Macromolecules* **1991**, *24*, 1567.
(6) Kim, S. S.; Han, C. D. *J. Rheol.* **1993**, *37*, 847.
(7) Kim, S. S.; Han, C. D. *Macromolecules* **1993**, *26*, 6633.
(8) Kim, S. S.; Han, C. D. *J. Polym. Sci., Polym. Phys. Ed.* **1994**, *32*, 371.
(9) Han, C. D.; Chang, S.; Kim, S. S. *Mol. Cryst. Liq. Cryst.* **1994**, *254*, 335.
(10) Chang, S.; Han, C. D. *Macromolecules* **1997**, *30*, 1656.
(11) Chang, S.; Han, C. D. *Macromolecules* **1997**, *30*, 2021.

(12) Kim, D.-O.; Han, C. D. *Macromolecules* **2000**, *33*, 3349.
(13) Hudson, S. D.; Lovinger, A. J.; Larson, R. G.; Davis, D. D.; Garay, R. O.; Fujishiro, K. *Macromolecules* **1993**, *26*, 5643.
(14) Baek, S. G.; Magda, J.; Larson, R. G.; Hudson, S. D. *J. Rheol.* **1994**, *38*, 1473.
(15) Gilmor, J. R.; Colby, R. H.; Hall, E.; Ober, C. K. *J. Rheol.* **1994**, *38*, 1623.
(16) Zhou, W. J.; Kornfield, J. A.; Ugaz, V. M.; Burghardt, W. R.; Link, D. R.; Clark, N. A. *Macromolecules* **1999**, *32*, 5581.
(17) Griffin, A. C.; Havens, S. J. *J. Polym. Sci., Polym. Phys. Ed.* **1981**, *19*, 951.
(18) Antoun, S.; Lenz, R. W.; Jin, J.-I. *J. Polym. Sci., Polym. Phys. Ed.* **1981**, *19*, 1901.
(19) Blumstein, A.; Thomas, O. *Macromolecules* **1982**, *15*, 1264.
(20) Percec, V.; Yourd, R. *Macromolecules* **1989**, *22*, 3229.
(21) Percec, V.; Tsuda, Y. *Macromolecules* **1990**, *23*, 3509.
(22) Ober, C. K.; Jin, J.-I.; Zhou, Q.; Lenz, R. W. *Adv. Polym. Sci.* **1984**, *59*, 103.
(23) Zhou, Q.; Lenz, R. W. *J. Polym. Sci., Polym. Chem. Ed.* **1983**, *21*, 3313.
(24) Furukawa, A.; Lenz, R. W. *Macromol. Chem., Macromol. Symp.* **1986**, *2*, 3.
(25) Kricheldorf, H. R.; Domschke, A.; Schwarz, G. *Macromolecules* **1991**, *24*, 1101.
(26) Shibaev, V. P.; Platé, N. A. *Adv. Polym. Sci.* **1984**, *60/61*, 173.
(27) McArdle, C. B., Ed.; *Side Chain Liquid Crystal Polymers;* Blackie and Sons: London, 1989.
(28) Percec, V.; Lee, M. *Macromolecules* **1991**, *24*, 1017.
(29) Percec, V.; Lee, M. *Polymer* **1991**, *32*, 2862.
(30) Percec, V.; Lee, M. *Macromolecules* **1991**, *24*, 4963.
(31) Percec, V.; Lee, M.; Ackerman, C. *Polymer* **1992**, *33*, 703.
(32) Komiya, Z.; Pugh, C.; Schrock, R. R. *Macromolecules* **1992**, *25*, 3609.
(33) Komiya, Z.; Pugh, C.; Schrock, R. R. *Macromolecules* **1992**, *25*, 6586.
(34) Komiya, Z.; Pugh, C.; Schrock, R. R. *Macromolecules* **1992**, *25*, 6593.
(35) Komiya, Z.; Schrock, R. R. *Macromolecules* **1993**, *26*, 1393.
(36) Imrie, C. T.; Karasz, F. E.; Attard, G. S. *Macromolecules* **1992**, *25*, 1278.
(37) Imrie, C. T.; Schleeh, T.; Karasz, F. E.; Attard, G. S. *Macromolecules* **1993**, *26*, 539.
(38) Imrie, C. T.; Karasz, F. E.; Attard, G. S. *Macromolecules* **1993**, *26*, 545.
(39) Imrie, C. T.; Karasz, F. E.; Attard, G. S. *Macromolecules* **1993**, *26*, 3803.
(40) Imrie, C. T.; Karasz, F. E.; Attard, G. S. *Macromolecules* **1994**, *27*, 1578.
(41) Craig, A. A.; Imrie, C. T. *J. Mater. Chem.* **1994**, *4*, 1705.
(42) Craig, A. A.; Imrie, C. T. *Macromolecules* **1995**, *28*, 3617.
(43) Kosaka, Y.; Kato, T.; Uryu, T. *Macromolecules* **1994**, 27, 2658.
(44) Kosaka, Y.; Uryu, T. *Macromolecules* **1994**, 27, 6286.
(45) Kosaka, Y.; Uryu, T. *Macromolecules* **1995**, *28*, 870.
(46) Hsiue, G.-H.; Wen, J.-S.; Hsu, C.-S. *Polym. Bull. (Berlin)* **1993**, *30*, 141.
(47) Bohnert, R.; Finkelmann, H. *Makromol. Chem. Rapid Commun.* **1993**, *14*, 139.
(48) Laus, M.; Bignozzi, M. C.; Angeloni, A. S.; Galli, G.; Chiellini, E. *Macromolecules* **1993**, *26*, 3999.
(49) Yamada, M.; Iguchi, T.; Hirao, A.; Nakahama, S.; Watanabe, J. *Macromolecules* **1995**, *28*, 50.
(50) Kawakami, Y.; Toida, K. *Macromolecules* **1995**, *28*, 816.
(51) Winkler, B.; Ungerank, M.; Stelzer, F. *Macromol. Chem. Phys.* **1996**, *197*, 2343.
(52) Lin, H.-C.; Lin, Y.-S.; Chen, Y.-T.; Chao, I.; Li, T.-W. *Macromolecules* **1998**, *31*, 7298.
(53) Zentel, R.; Wu, J. *Makromol. Chem.* **1986**, *187*, 1727.
(54) Fabre, P.; Veyssie, M. *Mol. Cryst. Liq. Cryst. Lett.* **1987**, *4*, 99.
(55) Colby, R. H.; Gillmor, J. R.; Galli, G.; Laus, M.; Ober, C. K.; Hall, E. *Liq. Cryst.* **1993**, *13*, 233.
(56) Kannan, R. M.; Kornfield, J. A. *Macromolecules* **1993**, *26*, 2050.
(57) Kannan, R. M.; Rubin, S. F.; Kornfield, J. A.; Boeffel, C. *J. Rheol.* **1994**, *38*, 1609.
(58) Rubin, S. F.; Kannan, R. M.; Kornfield, J. A.; Boeffel, C. *Macromolecules* **1995**, *28*, 3521.
(59) Grabowski, D. A.; Schmidt, C. *Macromolecules* **1994**, *27*, 2632.
(60) Berghausen, J.; Fuchs, J.; Richtering, W. *Macromolecules* **1997**, *30*, 7574.
(61) Colby, R. H.; Ober, C. K.; Gilmor, J. R.; Connelly, R. W.; Duong, T.; Galli, G.; Laus, M. *Rheol. Acta* **1997**, *36*, 498.
(62) Quijada-Garrido, I.; Siebert, H.; Friedrich, C.; Schmidt, C. *Rheol. Acta* **1999**, *38*, 3495.
(63) Quijada-Garrido, I.; Siebert, H.; Friedrich, C.; Schmidt, C. *Macromolecules* **2000**, *33*, 3844.
(64) Wewerka, A.; Viertler, K.; Vlassopoulos, D.; Stelzer, F. *Rheol. Acta* **2001**, *40*, 416.
(65) Wewerka, A.; Floudas, G.; Pakula, T.; Stelzer, F. *Macromolecules* **2001**, *34*, 8129.
(66) Lee, K. M.; Han, C. D. *Macromolecules* **2002**, *35*, 6263.
(67) Brown, H. C. *Hydroboration*; Benjamin: New York, 1962.
(68) Chung, T. C.; Raate, M.; Berluche, E.; Schulz, D. N. *Macromolecules* **1988**, *21*, 1903.
(69) Lee, K. M.; Han, C. D. *Macromolecules* **2002**, *35*, 760.
(70) Han, C. D. *Multiphase Flow in Polymer Processing*; Academic Press: New York, 1981.
(71) Kim, S. S.; Han, C. D. *Polymer* **1994**, *35*, 93.
(72) Han, C. D.; Baek, D. M.; Kim, J. K.; Chu, S. G. *Polymer* **1992**, *33*, 294.
(73) Han, J. H.; Feng, D.; Choi-Feng, C.; Han, C. D. *Polymer* **1995**, *36*, 155.
(74) Han, C. D.; Kim, J. *J. Polym. Sci., Polym. Phys. Ed.* **1987**, *25*, 1741.
(75) Han, C. D.; Kim, J.; Kim, J. K. *Macromolecules* **1989**, *22*, 383.
(76) Han, C. D.; Baek, D. M.; Kim, J. K. *Macromolecules* **1990**, *23*, 561.
(77) Han, C. D.; Jhon, M. S. *J. Appl. Polym. Sci.* **1986**, *32*, 3809.
(78) Han, C. D.; Kim, J. K. *Macromolecules* **1989**, *22*, 4292.
(79) Han, C. D.; Kim, J. K. *Polymer* **1993**, *34*, 2533.
(80) Onogi, S.; Asada, T. In *Proceesings of the 8th International Congress on Rheology*; Astarita, G., Marrucci, G., Nicolais, G., Eds.; Plenum: New York, 1980; Vol. 1, p 127.
(81) Ugaz, V. M.; Cinader, D. K.; Burghardt, W. R. *Macromolecules* **1997**, *30*, 1527.
(82) Kiss, G.; Porter, R. S. *J. Polym. Sci., Polym. Symp.* **1978**, *65*, 193.
(83) Kiss, G.; Porter, R. S. *J. Polym. Sci., Polym. Phys. Ed.* **1980**, *18*, 361.
(84) Navard, P.; Haudin, J. M. *J. Polym. Sci., Polym. Phys. Ed.* **1986**, *24*, 189.
(85) Grizzuti, N.; Cavella, S.; Cicarelli, P. *J. Rheol.* **1990**, *30*, 1293.
(86) Moldenaers, P.; Mewis, J. *J. Rheol.* **1986**, *30***,** 567.
(87) Baek, S.-G.; Magda, J. J.; Larson, R. G. *J. Rheol.* **1993**, *37***,** 1201.
(88) Baek, S.-G.; Magda, J. J.; Larson, R. G.; Hudson, S. D. *J. Rheol.* **1994**, *38***,** 1473.
(89) Marrucci, G.; Maffettone, P. L. *Macromolecules* **1989**, *22*, 4076.
(90) Cocchini, F.; Aratari, C.; Marrucci, G. *Macromolecules* **1990**, *23*, 4446.
(91) Larson, R. G. *Mcromolecules* **1990**, *23*, 3983.
(92) Ugaz, V. M.; Burghardt, W. R. *Macromolecules* **1998**, *31*, 8474.
(93) Zhou, W.-J.; Kornfield, J. A.; Burghardt, W. R. *Macromolecules* **2001**, *34*, 3654.
(94) Gouinlock, E. V.; Porter, R. S. *Polym. Eng. Sci.* **1977**, *17*, 534.
(95) Han, C. D.; Baek, D. M.; Kim, J. K.; Ogawa, T.; Sakamoto, N.; Hashimoto, T. *Macromolecules* **1995**, *28*, 5043 and references therein.
(96) Ugaz, V. M.; Burghardt, W. R.; Zhou, W.-J.; Kornfield, J. A. *J. Rheol.* **2001**, *45*, 1029.
(97) Han, C. D.; Chang. S. *J. Rheol.* **1994**, *38*, 13.
(98) Mather, P. T.; Jeon, H. G.; Han, C. D.; Chang, S. *Macromolecules* **2000**, *33*, 7594.
(99) Donald, A. M.; Viney, C.; Windle, A. H. *Polymer* **1983**, *24*, 155.
(100) Viney, C.; Donald, A. M.; Windle, A. H. *J. Mater. Sci.* **1983**, *18*, 1136.
(101) Donald, A. M.; Windle, A. H. *J. Mater. Sci.* **1983**, *18*, 1143.
(102) Zachariades, A. E.; Navard, P.; Logan, J. P. *Mol. Cryst. Liq. Cryst.* **1984**, *110*, 93.
(103) Navard, P.; Zachariades, A. E. *J. Polym. Sci., Polym. Phys. Ed.* **1987**, *25*, 1089.
(104) Takeuchi, Y.; Shuto, Y.; Yamamoto, F. *Polymer* **1988**, *29*, 605.
(105) Han, C. D.; Chang, S.; Kim, S. S. *Macromolecules* **1994**, *27*, 7699.
(106) Chang, S.; Han, C. D. *Macromolecules* **1996**, *29*, 2383.
(107) Tang, B. Z.; Kong, X.; Wan, X.; Peng, H.; Lam, W. Y.; Feng, X.-D.; Kwok, H. S. *Macromolecules* **1998**, *31*, 2419.

MA030303O